

**NASA Contractor Report 187519**

**ICASE Report No. 91-17**

# ICASE

## PROBABILITY DISTRIBUTION FUNCTIONS IN TURBULENT CONVECTION

**S. Balachandar**

**L. Sirovich**

Contract No. NAS1-18605

February 1991

Institute for Computer Applications in Science and Engineering  
NASA Langley Research Center  
Hampton, Virginia 23665-5225

Operated by the Universities Space Research Association



National Aeronautics and  
Space Administration

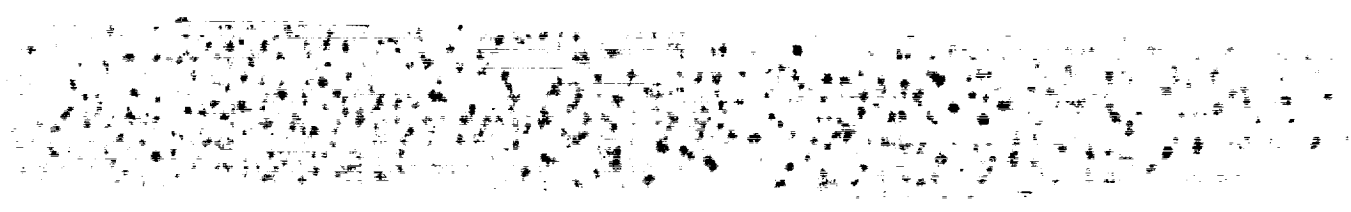
Langley Research Center  
Hampton, Virginia 23665-5225

(NASA-CR-187519) PROBABILITY DISTRIBUTION  
FUNCTIONS IN TURBULENT CONVECTION Final  
Report (ICASE) 41 p CSCL 200

N91-21453

Unclas  
0003351

G3/34



# Probability Distribution Functions in Turbulent Convection

S. Balachandar\* and L. Sirovich<sup>1</sup>

Center for Fluid Mechanics

Brown University

Providence, RI 02912

\* Theoretical and Applied Mechanics Department

University of Illinois

Urbana, IL 61801

## ABSTRACT

Results of an extensive investigation of probability distribution functions (pdfs) for Rayleigh-Bénard convection, in the hard turbulence regime, is presented. It is seen that the pdfs exhibit a high degree of internal universality. In certain cases this universality is established within two Kolmogorov scales of a boundary. A discussion of the factors leading to universality is presented.

---

<sup>1</sup>Research was supported in part by the National Aeronautics and Space Administration under NASA Contract No. NAS1-18605 while the author was in residence at the Institute for Computer Applications in Science and Engineering (ICASE), NASA Langley Research Center, Hampton, VA 23665-5225.

10. The following information is taken from the financial statements of a company for the year ended 31st December 2018:

Revenue 1,200,000  
Cost of sales 750,000  
Gross profit 450,000

Required: Calculate the gross profit margin and the gross profit ratio.

# 1 Introduction

Probability distribution functions (pdfs) long have been of importance in discussing turbulent flows (see Pope<sup>1</sup> for a comprehensive review to 1985). They serve as a valuable tool in presenting data and give valuable insights into range of behavior. Recent work<sup>2-5</sup> has placed a new emphasis on their study in turbulent flows. Direct numerical simulations<sup>6-9</sup> and improved experimental techniques<sup>10-12</sup> have permitted more detailed pdfs, and allow us to go well beyond such low order moments as variances  $\sigma$ , skewness  $s$  and flatness  $f$ , common in the statistical description of turbulent flows. Part of the recent interest in pdfs is due to the experiments of the Chicago group,<sup>10-12</sup> and in particular to the *exponential* tails they observed for the pdfs of temperature fluctuations. The wide *tails* of such pdfs *underline the essential role that intermittency* plays in turbulence phenomena. However, earlier investigations also led to such exponential distributions<sup>13-15</sup>.

On the theoretical side, Sinai and Yakhot<sup>2</sup> considered the pdf of a passive scalar and made remarkable progress in describing the limiting distribution function. Subsequent to this, Yakhot and coworkers<sup>3,16</sup> extended this approach and presented arguments leading to exponential pdfs for temperature fluctuations and vorticity. Kraichnan has also made a notable extension to this approach.<sup>5</sup> More recently Kraichnan<sup>17,18</sup> has produced a relatively simple *closure* model based on the mechanisms at work in fluid flow which lead to wide skirted pdfs.

In this paper we present the results of an extensive study of pdfs as generated in a computational investigation of the Rayleigh-Bénard (R-B) convection problem. The present results are based on a substantially longer simulation than was considered in our earlier publications.<sup>6,7</sup> For purposes of comparison we estimate the turnover time by

$$(1) \quad \tau = H/q_{rms}$$

where  $H$  is the height of the computational cell and  $q_{rms}$  represents the rms speed. In such terms our earlier work was based on 4.65 turnover times while the present study is based on 41.7 turnover times.

The specification of the problem as well as the details of the calculation appear in our earlier work<sup>6,7</sup>. In brief, we simulate turbulent thermal convection as described by the Boussinesq equations<sup>19</sup>. The vertical coordinate is denoted by  $z$  and the horizontal by  $x$  and  $y$ . The horizontal planform is a square and the aspect ratio (width to height) is  $2\sqrt{2}$ . The Rayleigh number is  $.98 \times 10^4$  times the critical value, which places the simulation in the range of hard turbulence in the terminology of the Chicago group.<sup>10-12</sup> The velocity satisfies slip boundary conditions on the impermeable horizontal boundaries and temperature is specified on these walls. Periodic boundary conditions are imposed in both horizontal directions.

The calculation uses 96 equal grid spacing in the vertical direction, with a like number in each of the horizontal directions. Since the Nusselt number,  $Nu$ , is roughly 23 for this calculation and since

$$(2) \quad Nu \approx \frac{H}{2\delta},$$

where  $\delta$  is the thickness of the thermal sub-layer, two grid spacings lie in the sublayer. (The sub-layer thickness is also a measure of the Komogorov scale.) These few facts are useful in interpreting the material that follows since various quantities will be specified by their vertical grid spacing locations.

As will be seen the pdfs exhibit a remarkable degree of universality. By universality we mean the unanticipated lack of dependence on strongly inhomogeneous directions. As discussed in Section 6 the same universality is expected to extend to other convection problems if the pdfs are suitably normalized.

## 2 Preliminary Considerations

In general if  $\alpha$  represents a dependent variable, then we will denote by

$$(3) \quad P_\alpha = P \left( \frac{\alpha - \bar{\alpha}}{\sqrt{(\alpha - \bar{\alpha})^2}} \right) = P(\hat{\alpha}),$$

the pdf which will be plotted in our figures. The bar signifies that the quantity has been averaged in time as well as over a horizontal plane. As previously reported for Bénard convection<sup>6,7</sup> temperature pdfs vary considerably in the vertical direction, Figure 1 shows the pdf of temperature fluctuation,  $T'$ , at six different elevations. (See the cited reference for more details of the calculation and notation.) The temperature pdf at the edge of the thermal sub-layer ( $z = 2/96$ ) though not symmetric, has skewness close to zero. Above the bottom sub-layer ( $z = 7/96, 16/96$ , and  $26/96$ ) the pdfs exhibit a peak corresponding to a small negative value and a long positive tail, resulting in significant positive skewness. This indicates the existence of hot thermal plumes near the bottom boundary and at the mid-plane the pdf is symmetric. Figure 2 shows the comparable pdfs for the horizontal velocity  $u$  and vertical velocity  $w$ . The parabolic shape of the  $u$  pdf in this log-linear plot indicates the Gaussian nature of the distribution. At the mid-plane the pdf of  $w$  exhibits a similar Gaussian nature, whereas below the midplane the pdf of  $w$  is positively skewed similar to the temperature pdfs but to a much lesser extent.

In our earlier papers we confirmed the existence of an exponential range to the pdf for fluctuations in temperature in the midplane as first exhibited by the Chicago group. This result was based on less than three log units range in the pdf. With the increased database, we now have reliable data for a range of almost six log units as exhibited in Figure 1. While the pdf in the midplane is still *fit* by an exponential over the first two to three log units the overall picture is quite different. The reason for the sharp down turn in the

tails of the pdf is easy to understand. Since the temperature fluctuations are bounded below and above by the wall temperatures, the *skirts* of the pdf,  $P(\hat{T}')$ , must terminate at finite values. This tendency is clearly exhibited by the midplane pdf shown in Figure 1. A brief summary describing the shape of the  $P(\hat{T}')$  at the midplane is: (1) first, analytical considerations dictate that the pdf must be rounded at the center; (2) next, this is followed by wide skirts, fit by an exponential, and which indicate relatively large fluctuations; (3) finally, limited temperature fluctuations dictated by the wall temperatures force a rapid falloff of the skirts.

In viewing the preceding pdfs and those to be presented later it is important to keep in mind the symmetries of the problem. This is especially true of the pdfs measured in the midplane of the cell  $z = 48/96$ , since some pdfs become symmetric only in the midplane. As has been shown, the problem under discussion has a sixteen-fold symmetry group<sup>20</sup>. We *have not* made use of this to extend the database (and thus sharpen the pdf curves) but instead have verified these symmetries to support the correctness of data. (E.g.  $P(\hat{v})$ , not shown, is virtually identical to  $P(\hat{u})$ , Figure 2(a).) In considering the pdfs it is useful to split these into two classes. Those that must have symmetric distributions as a result of an inherent symmetry and those for which there is no *a priori* symmetry requirement. In general, if we consider a pdf  $P(\hat{\alpha})$ , and if there exists an admissible transformation of the group,  $G$ , such that

$$(4) \quad G\alpha = -\alpha$$

then this implies that

$$(5) \quad P(\hat{\alpha}) = P(-\hat{\alpha}).$$

Consider for example the horizontal velocity  $u$ . Under reflection in the plane  $x = 0$ ,  $u \rightarrow -u$ , and hence  $P(\hat{u})$  is symmetric for all  $z$  values. This



is clearly indicated in Figure 2a. Alternately, both the vertical velocity  $w$ , and the temperature fluctuation  $T'$  go into their negatives under reflection in the midplane, *but not elsewhere*. Thus their mid-plane pdfs should be symmetric and as seen in Figures 1 and 2(b), this is the case. However no group operation produces (4) at other  $z$  elevations and there is no reason for these pdfs to be symmetric for other values of  $z$ . This is borne out by Figures 1 and 2(b).

We can carry this line of reasoning somewhat further and consider  $w_z$  and  $T'_z$ , neither of which have a group operation leading to (4). Figures 3a and 3b show the pdfs for each of these quantities. As can be seen the corresponding pdfs show no symmetry at any  $z$  values. This can be given a physical interpretation. Away from the two thin sub-layers near the top and the bottom boundaries the pdfs are negatively skewed. To see this consider a parcel of fluid located at some height  $z'$  travelling up. Since the vertical velocity and temperature fluctuations are well correlated, the probability that this parcel of fluid has positive temperature fluctuation is high. After a small time interval the fluid parcel will be at a higher elevation  $z' + \delta z'$  surrounded by relatively colder fluid. Therefore the probability that this parcel will accelerate up ( $w_z > 0$ ) and contribute larger temperature fluctuation ( $T'_z > 0$ ) is high. Similarly if we consider a parcel of fluid with negative temperature fluctuation moving down, the probability that the parcel will accelerate down ( $w_z > 0$ ) with larger temperature fluctuation ( $T'_z > 0$ ) is large. Therefore both  $w_z$  and  $T'_z$  show a peak in their probability distribution at a (small) positive value and this peak is compensated by a less steeper negative tail, in order to yield zero mean values. For the  $P(\hat{w}_z)$  this negative tail can be associated with the less probable event of rapid deceleration of both the up moving cold parcel of fluid and the down moving warm parcel of fluid. In other words, mild acceleration up or down is more probable than mild deceleration, but rapid deceleration (up or down) is more probable than rapid acceleration. Similar interpretations can be given for the gradient of the tem-

perature fluctuations as well, and in general the pdf of a quantity provides us with a view of its range of behavior.

For comparison with the pdfs of Figure 3, we consider  $u_z$  which has a symmetry leading to (5) for all  $z$ . The corresponding pdf is shown in Figure 4. This clearly indicates the symmetry but in addition shows a remarkable degree of universality in the  $z$ -direction. Such universality will be encountered for the majority of the pdfs which will be presented below. Further discussion of this unexpected property will be presented in the following sections.

### 3 Probability Distribution Functions

As already seen in Figure 4 the pdf of  $u_x$  (or equivalently  $v_x$ ) exhibits a surprising universality across the convective cell. To explore this property further we present, in Figure 5, the components of vorticity. The pdfs for the horizontal components  $\Omega_1$  and  $\Omega_2$  are virtually identical, only  $\Omega_1$  is shown, and in addition exhibit a high degree of universality. Vertical vorticity,  $\Omega_3$ , on the other hand shows a significant departure from universality. All vorticity components lead to pdfs which satisfy (4), either through reflection in a plane of constant  $x$  or  $y$ .

Given that mechanisms are at work that force universality, we should expect in general that boundaries will produce significant departures from universality. To contrast the results of the pdfs for the horizontal and vertical components we recall that

$$(6) \quad \Omega_1 = \left( \frac{\partial w}{\partial y} - \frac{\partial v}{\partial z} \right),$$

$$(7) \quad \Omega_3 = \left( \frac{\partial v}{\partial x} - \frac{\partial u}{\partial y} \right).$$

It follows from the boundary conditions for this particular R-B convection problem<sup>19</sup> that  $\Omega_1 \equiv 0$  (and  $\Omega_2 \equiv 0$ ) at a wall, while  $\Omega_3$  is unrestricted at a wall. As a general principle one should expect that all *permissible* fluctuations will appear in the corresponding pdf with an appropriate probability. This can be seen in Figure 5. Thus  $\Omega_3$  which is unrestricted at the boundary has a wide skirt at  $z = 2/96$ , while  $\Omega_1$  which is restricted at the wall can only develop a slight skirt in the neighborhood of the wall  $z = 2/96$ . As a result universality does not appear in  $P(\hat{\Omega}_3)$  until we approach the central region, where the pdf is fit by the universal curve. On the other hand universality is quickly achieved for  $P(\hat{\Omega}_1)$  and  $P(\hat{\Omega}_2)$ . It should be noted that in the central region the pdf of all three components of vorticity are well fit by the same

exponential over at least three decades. Further the pdfs of those velocity derivatives that constitute the three components of vorticity ( $u_y, u_x, v_x, v_z, w_x$  and  $w_y$ ), coincide with the above exponential distribution (for example see Figure 4).

We have already seen in Figures 1 and 3, examples of pdfs that show a strong departure from universality. For each of these pdfs the quantity in question does not satisfy the symmetry property (4) except possibly at the center plane. Both  $u_x$  and  $v_y$  are linked to  $w_z$  through the continuity equation. Since neither of these quantities have a transformation leading to (5), their pdfs lack universality. The pdfs for  $u_x$  and  $v_y$  closely resemble those shown in Figure 3(a) and are not presented here. (Only the pdf of  $w_z$  at  $z = 2/96$  is significantly different.) [Although  $u_x$  and  $v_y$  are identically distributed, they are correlated, since the convolution of  $P(\hat{u}_x)$  with itself does not produce  $P(\hat{w}_z)$ .]

The pdfs for  $w_x$ , with high accuracy lie on those of  $\Omega_1$ , Figure 5(a). By contrast with the pdf in  $w$ , Figure 2(b), this is universal except very near the wall. Thus taking a derivative of  $w$ , which then leads to a symmetrizing transformation, (4), produces a quick transition to universality. In addition, the value of  $w_x$  is pinned to be equal to zero at both the top and bottom boundaries. This transition to universality is less true for  $T'_x$ , the pdf of which is shown in Figure 6. We recall, however, that the pdf of  $T'$  itself, Figure 1, is far less universal and significantly more skewed than the pdf of  $w$ , Figure 2(b).

In general it can be observed that temperature statistics obey universality over a narrower region near the midplane than their velocity counterpart. This reluctance towards universality can be, at least partially, attributed to the highly intermittent nature of temperature and its derivative signals. For example, at the midplane while the pdf of  $u$  and  $w$  are Gaussian the pdf of  $T'$  is exponential and while the pdf of vorticity is exponential the pdf of  $T'_x$  is flatter than an exponential.

## 4 PDFS for Higher Derivatives

By taking derivatives of flow variables we emphasize the smaller scales. It is a widely held view that small scales *forget* their large scales origins. This concept lies at the heart of the  $-5/3$  Kolmogorov range<sup>21</sup> and of the exponential dissipative range<sup>22</sup>. Both these energy ranges represent universal behavior of turbulent flows. Thus, as derivatives of flow quantities are increased their pdfs depend more heavily on the higher wavenumbers and a tendency towards universality should be expected. Pdfs of derivatives say something about distributions in small eddies, the higher the derivative the smaller the dominant eddy. What must be regarded as remarkable is that even pdfs of first derivatives show universality. It would appear that more than the above mentioned universal ranges are at work in producing universality, and very probably that dynamics is important in establishing at least some of the universal features.

In this section we consider the effect of taking additional derivatives of flow quantities on the corresponding pdfs. In Figures 7-9 we exhibit a selection of second derivatives of flow quantities. These show a higher degree of universality than their first derivative counterparts. Before commenting on these in detail, we observe that all the pdfs shown in these figures exhibit a flared out skirt and are no longer fit by a simple exponential. To account for this effect, we refer to an argument given sometime ago by Kraichnan<sup>23</sup> which demonstrates that greater intermittency is to be expected as the wavenumber is increased. His argument is largely independent of Reynolds number. Thus in viewing pdfs of higher derivatives of flow quantities we should expect increasing intermittency and hence wider flaring skirts in the pdfs.

In Figures 7(a) and 7(b) we show the pdfs for  $u_{zz}$  and  $u_{yz}$  both of which exhibit strong universality. On the other hand pdfs for  $u_{yy}$  shown in Figure 7(c) exhibit some departure from universality.  $u_{yz}$  is identically equal to zero at both boundaries, due to the stress-free boundary condition, therefore a

strong tendency towards universality can be expected. Though the boundary condition for the other three quantities are not prescribed, variations in  $u_{zz}$  will be small since it is the vertical gradient of  $u_z$  which is identically equal to zero at boundaries. As seen earlier, functions that are fixed at the boundaries quickly attain universality and within the universal regime the vertical gradients as well as the horizontal gradients can be expected to be bounded and exhibit strong universality. On the contrary, both  $u_{yy}$  and  $u_{xy}$  are neither fixed at the boundary nor do they represent the derivative of a quantity which exhibit universality.

We do not show the three pdfs corresponding to  $w_{xx}$ ,  $w_{zz}$  and  $w_{xz}$ , since they virtually lie on the universal curve of Figure 7(b). The pdfs of the first two have no transformation under which (5) holds. Symmetry is nevertheless established. This confirms that skewness is primarily a property of large scale structures.<sup>9</sup> Both  $w_{xx}$  and  $w_{zz}$  ( by continuity) are restricted to be zero at the boundary, whereas  $w_{xz}$  is the vertical derivative of the universal function  $w_x$ . Therefore all three pdfs show universality and to excellent approximation fall on the same curve, Figure 7(b). In Figure 8 we show pdfs for  $T'_{xx}$  and  $T'_{zz}$ . The pdfs for the last quantity does not have a symmetrizing transformation leading to (4). Nevertheless except near the wall for  $P(\overline{T'_{zz}})$  the pdfs are symmetric and exhibit a tendency towards universality. This is even more true for  $T'_{xx}$  which also does not have a symmetrizing transformation but has pdfs very well fit by Figure 8(a).

Thus we conclude that whatever the mechanism forcing universality, as might be expected, it is more effective on higher derivatives.

## 5 Other Mean Quantities

Figure 9 contains plots of  $T'_{rms}, u_{rms}, w_{rms}$ , as well as  $\langle WT' \rangle$  (and its covariance) and  $\frac{d}{dz} \langle T' \rangle$ . In certain instances for a range of  $z$ , the curves are well fit by power laws and this has been indicated. Arguments leading to power law dependence are similar to those leading to the inertial sublayer (log-layer) for turbulent wall bounded flows.<sup>24</sup> In brief once away from the diffusive layers adjacent to a wall the only available length scale is the distance to the boundary. Prandtl<sup>25</sup> applied this to the convection problem and one finds<sup>24,26</sup>

$$(8) \quad T'_{rms} \propto z^{-1/3}, w_{rms} \propto z^{1/3}; \frac{dT'}{dz} \propto z^{-4/3}$$

in this region.  $T'_{rms}$  and  $w_{rms}$  are the rms temperature and vertical velocity fluctuations (Kraichnan,<sup>27</sup> also using mixing length theory, has considered in detail the case in which the  $Pr$  number is allowed a wide range of values.) A simple argument which leads to (8) is that since in the inviscid region the convective heat transport

$$(9) \quad \overline{wT'} = H_0$$

is a constant, this implies that  $w$  and  $T'$  scale reciprocally with  $z$ . Thus, in the vertical momentum equation the lead terms are

$$(10) \quad w \frac{\partial w}{\partial z} \propto T'$$

from which the scaling in (8) follows.

While  $T'_{rms}$  does show a sensible range for a  $(-1/3)$ -power, the same is not true for  $w_{rms}$ . Though the convective heat transport  $\langle wT' \rangle$  and (the covariance  $\langle wT' \rangle / w_{rms} T'_{rms}$ ) are constant across the layer ( $.20 \leq z \leq .35$ ) except near the boundary,  $w$  does not scale reciprocally since the region over which  $T' \propto z^{1/3}$  ( $.05 < z < .2$ ) falls closer to the boundaries. We also

note that  $d\overline{T}/dz$ , does not follow a  $-4/3$ -power. Townsend<sup>28,29</sup> observed a  $-2$  power, indicated as a dashed line in the Figure, a value also given by Carroll<sup>30</sup> and in a computation by Eidson et al.<sup>31</sup> This value was first proposed by Malkus<sup>32</sup> from theoretical arguments. However we point out that a  $-9/4$  power, the continuous straight line of the Figure, is a better fit to the calculation.

The lack of a consistent universal scaling regime is reminiscent of the situation for boundary layer flows, where an argument similar to that leading to (8) produces the *log layer* for the mean velocity<sup>33</sup>. However as has been known for some time, not all quantities follow the universal scaling. To account for the lack of universality Townsend<sup>34</sup> and later Bradshaw<sup>35</sup> postulated the notion of *active* and *inactive* portions of the flow. In their explanation they invoke the idea of large (integral scale) eddies entering the boundary regions at infrequent times and marring the universality of some quantities.

In the present case, the underlying scaling arguments assume a semi-infinite domain in the vertical direction without horizontal wind,<sup>26</sup> and so might be thought to be applicable outside the dissipative sublayer at a wall. Recent experiments by the Chicago group indicate a sustained symmetry breaking *wind*. Also for the numerical simulations already discussed<sup>6,7</sup>, the roll motions act as a winds since their time scale is of relatively long duration although they have zero mean. In any event this more general case changes the above dimensional reasoning and is treated in Monin and Yaglom<sup>26</sup> who find general classes of possible functional dependences. We do not pursue this further since scaling does not appear to be a dominant effect.

Since all the pdfs considered are given in the normalization, (3), it is of interest to present the remaining variances of the quantities considered with respect to their variation in the vertical direction,  $z$ . The rms fluctuation of the three components of vorticity are plotted in Figure 10. Figures 11, 12



and 13 show the rms fluctuation for the first and second derivative quantities. Since pdfs of the raw variables follow from these plots this completes the single point probabilistic description of all the relevant quantities.

While scaling does not appear to account for the universality another feature of the pdfs does help explain the collapse of pdfs onto universal curves. We observe that the above symmetric pdfs are well approximated by the family of curves

$$(11) \quad P(\alpha) = C e^{-\frac{|\alpha|^p}{k}},$$

where  $C = C(p, k)$  is easily chosen so that there is unit area under the curve.  $p = 2$  corresponds to a Gaussian distribution,  $p = 1$  corresponds to an exponential distribution and  $p$  less than one indicates a flatter *intermittent* distribution. All the even moments of this distribution depend on  $p$  and  $k$ , while the odd moments are identically equal to zero. Closer to the boundaries the distributions are intermittent and the pdfs are flared out corresponding to  $p$  less than 1. As universality is approached the value of  $p$  decreases and in the universal regime since the level of intermittency can be expected to be uniform in the value of  $p$  i.e. it will be independent of the vertical location. Although  $k$ , which measures the width or the standard deviation of the pdf, can vary in the universal regime for the raw variables, once the raw variables are normalized by the rms fluctuation the value of  $k$  is dictated to be  $\left[ \frac{\Gamma(\frac{1}{p})}{\Gamma(\frac{3}{p})} \right]^{p/2}$  so that the normalized standard deviation is unity. Therefore in the universal regime  $p$  and  $k$  (which now depends only on  $p$ ) are constants. Therefore as long as the level of intermittency (or  $p$ ) reaches an asymptotic value, indicating universality, the collapse of the normalized pdfs can be explained. As already mentioned the approach to universality is rapid in the case of variables that are fixed at the boundaries.

## 6 Concluding Remarks

An overall survey of the pdfs that have been exhibited leads one to believe that there is an active mechanism forcing the pdfs toward universal form. Both the degree to which this is true and the resulting shape of the pdf depend on the dominant relevant *eddy size* i.e. on the number of derivatives being considered. In general the smaller the eddies, the more quickly is universality established, and the more intermittent (flared skirts) the shape of the pdf. As has been observed by She et al<sup>9</sup> skewness is essentially a large scale property, while *flatness* is a small scale effect.

As might be expected the presence of boundaries mars universality and wide departures from universal behavior can be expected in the neighborhood of a boundary. A boundary can act in two extremely different ways. It can *pin down* a fluctuation. E.g.  $w, T', w_x, u_x, \dots$  are all restricted to vanish at a boundary. On the other hand  $\Omega_3, T'_x, w_x, u_y, u_x, \dots$  are all unrestricted in that any fluctuation in those quantities is permitted at the boundary. Another important ingredient in determining the form of a pdf is symmetry. If a transformation of the form (4) is applicable then a symmetric pdf results. In certain instances this is only achieved at the midplane, e.g.  $w$  and  $T'$ . While in other cases symmetric pdfs must be obtained (assuming that there exists sufficient data) at all elevations, e.g.  $u, w_x, u_x, \dots$

As a general rule, at a boundary, and in its neighborhood, if there is no restriction imposed on the quantity, one should expect all manner of possible fluctuations to appear. This helps to explain why for example,  $P(\hat{\Omega}_3)$  has relatively wide skirts in the neighborhood of the boundary, and as a result shows a slower tendency to universality. By comparison  $u_x$  must be zero at a boundary and thus does not develop wide skirts in the neighborhood of a boundary. Unlike  $P(\hat{\Omega}_3)$ ,  $P(\hat{u}_x)$  tends very quickly to a universal form, Figure 4.

The cases of  $P(\hat{T}')$  and  $P(\hat{w})$  are of interest to consider from the perspec-

tive of the present discussion. In both instances the quantity in question is forced to vanish at the boundary. This however has little effect in restricting the corresponding pdf. Although each must be symmetric in the midplane, this is not true elsewhere and the passage to the symmetric pdf is difficult to characterize.

The mechanism which is responsible for the tendency towards universality is not obvious. Kraichnan<sup>5,18</sup> has produced a simple heuristic model of intermittency based on a closure approximation which exhibits independence of  $Re$ . This may be indicative of the processes at work and which bring about universality. Further investigation of this effect is clearly indicated.

While our deliberations are based on the computation of R-B convection, at one value of  $Ra$ , it seems clear that they should be generalize to other flow geometries and other values of the control parameter. The approach to universality which we have followed in terms of the vertical distance from a wall is doubtless better expressed in terms of a *wall normalized variable*. For channel or boundary layer flows this would be the usual wall normal coordinate, while in the present case  $z/\delta$  is the suitable variable. When the pdfs are expressed in such terms we anticipate that universality will also hold with varying control parameters. A study of available channel flow data strongly indicates universal forms for the corresponding pdfs.<sup>37</sup>

### Acknowledgement

The authors are grateful to Bruce Knight for many helpful discussions. The work reported here was supported by DARPA-URI N00014-86-K0754.

### References

1. S.B. Pope, Prog. Ener. Combust. Sci. 11, 119 (1985)
2. Ja. G. Sinai and V. Yakhot, Phys. Rev. Lett. 63, 1962 (1989)

3. V. Yakhot, Phys. Rev. Lett. **63**, 1965 (1989).
4. H. Chen, S. Chen and R. Kraichnan, Phys. Rev. Lett. **63**, 2657 (1989)
5. R. H. Kraichnan, Models of intermittency in hydrodynamic turbulence, Phys. Rev. Lett. **65**, 575 (1990).
6. L. Sirovich, S. Balachander and M.R. Maxey, Phy. Fluid A **1**, 1911 (1989)
7. S. Balachandar, M.R. Maxey and L. Sirovich, J. Sci. Comp. **4** (2), 219-236 (1989)
8. R.M. Kerr, J. Fluid Mech. **153**, 31 (1985).
9. Z-S. She, E. Jackson and S.A. Orszag, J. Sci. Comp. **3**, 407 (1988).
10. F. Heslot, B. Castaing and A. Libchaber, Phys. Rev. A **36**, 5870 (1987)
11. B. Castaing, G. Gunaratine, F. Heslot, L. Kadanoff, A. Libchaber, S. Thomas, X.Z. Wu, S. Zaleski and G. Zannetti, J. Fluid Mech. **204**, 1 (1989)
12. M. Sano, X.Z. Wu and A. Libchaber, Phys. Rev. A **40**, (11) 6421-6430 (1989)
13. K.R. Sreenivasan, R. Narashima and A. Prabhu, J. Fluid Mech. **137**, 251 (1983)
14. F.N. Frenkiel, P.S. Klebinoff and T.T. Huang, Phys. Fluid **22**, 1606 (1979)
15. F. Anselmet, Y. Gagne, E.J. Hopfinger, R.A. Antonia, J. Fluid Mech. **140**, 63 (1984)
16. V. Yakhot, S.A. Orszag, S. Balachandar, E. Jackson, Z.-S. She, L. Sirovich, Phenomenological theory of probability distribution functions in turbulent flows, Proceedings of the Sixth Beersheba Seminar, Jerusalem, Feb. 1990 (H. Branover, ed.), AIAA.
17. R. Kraichnan in *New Perspectives in Turbulence* (L. Sirovich, editor) Springer Verlag (1990)

18. R. Kraichnan, Intermittent turbulence from closures, Proceedings of the Sixth Beersheba Seminar, Jerusalem, Feb. 1990 (H. Branover, ed.), AIAA.
19. P.G. Drazin and W.H. Reid, *Hydrodynamic Stability*, Cambridge University Press (1981)
20. L. Sirovich, Quar. Appl. Math. XLV, 572 (1987)
21. A.N. Kolmogorov, C. R. Acad. Sci. (USSR) 30 301 (1941)
22. C. Foias, O. Manley and L. Sirovich Phys. Fluids A 2, 464 (1990)
23. R. Kraichnan, Phys. of Fluids 10, 2080 (1967)
24. A.S. Monin and A.M. Yaglom, *Statistical Fluid Mechanics*, Vol. 2, MIT Press, Cambridge (1975)
25. L. Prandtl, Beitr. Phys. Atmos. 19, 188 (1932)
26. C.H.B. Priestly, Aust. J. Phys. 7, 176 (1954)
27. R. Kraichnan, Phys. of Fluids 5, 1374 (1962)
28. A.A. Townsend, J. Fluid Mech. 5 209 (1959)
29. D.B. Thomas and A.A. Townsend, J. Fluid Mech. 2, 473 (1957)
30. J.J. Carroll, J. Atmos. Sci. 33, 642 (1976)
31. T.M. Eidson, M.Y. Hussaini and T.A. Zang, in *Notes on Numerical Fluid Mech.* 15, 188. Vieweg, Braunschweig (1986)
32. W.V.R. Malkus, Proc. Roy. Soc. (London) A 225, 196 (1954)
33. H. Tennekes and J. Lumley, *A First Course in Turbulence*, MIT Press, Cambridge, (1972)
34. A.A. Townsend, J. Fluid Mech. 11, 97 (1961)
35. J. Bradshaw, J. Fluid Mech 30, 241 (1967)
36. P.K. Yeung and S.B. Pope, Jour. Fluid Mech. 207, 531 (1989)
37. S. Balachandar, K. Breuer, R. Handler and L. Sirovich, Probability distribution function for turbulent channel flow. To be submitted to Physics of Fluids.

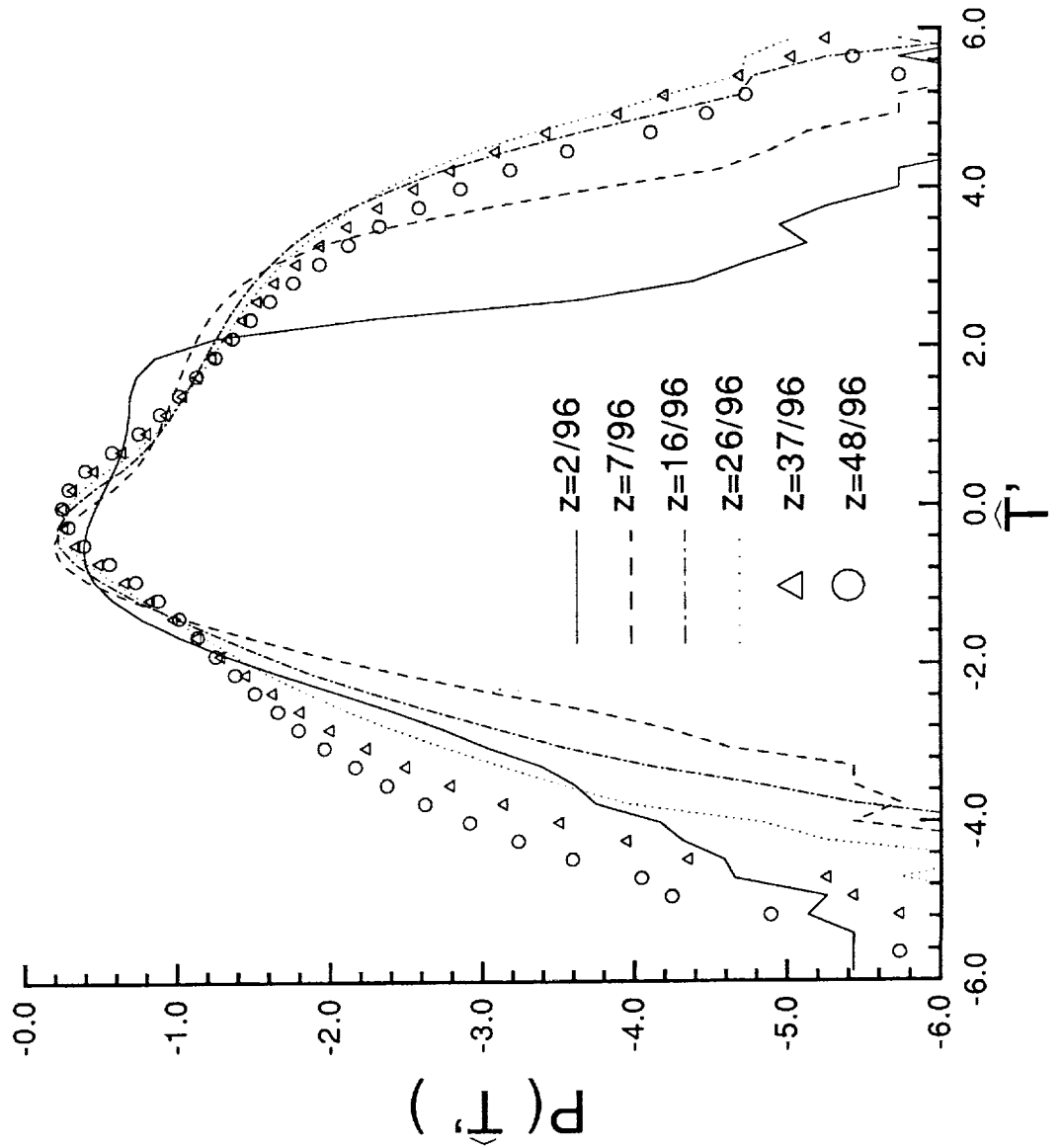


Figure 1: Probability distribution function of normalized temperature fluctuation  $T' = \frac{T' - \overline{T'}}{\sqrt{\overline{T'^2 - \overline{T'}^2}}$  at six different heights from the bottom boundary.  $z = 2/96$  is at the edge of the bottom thermal sub-layer.  $z = 7/96$  is in the region of hot thermal plumes and  $z = 16/96$  is roughly at the edge of the plume region.  $z = 26/96, 37/96$  and  $48/96$  are in the turbulent core. The results corresponding to the top half can be extended from the bottom half based on symmetry conditions.

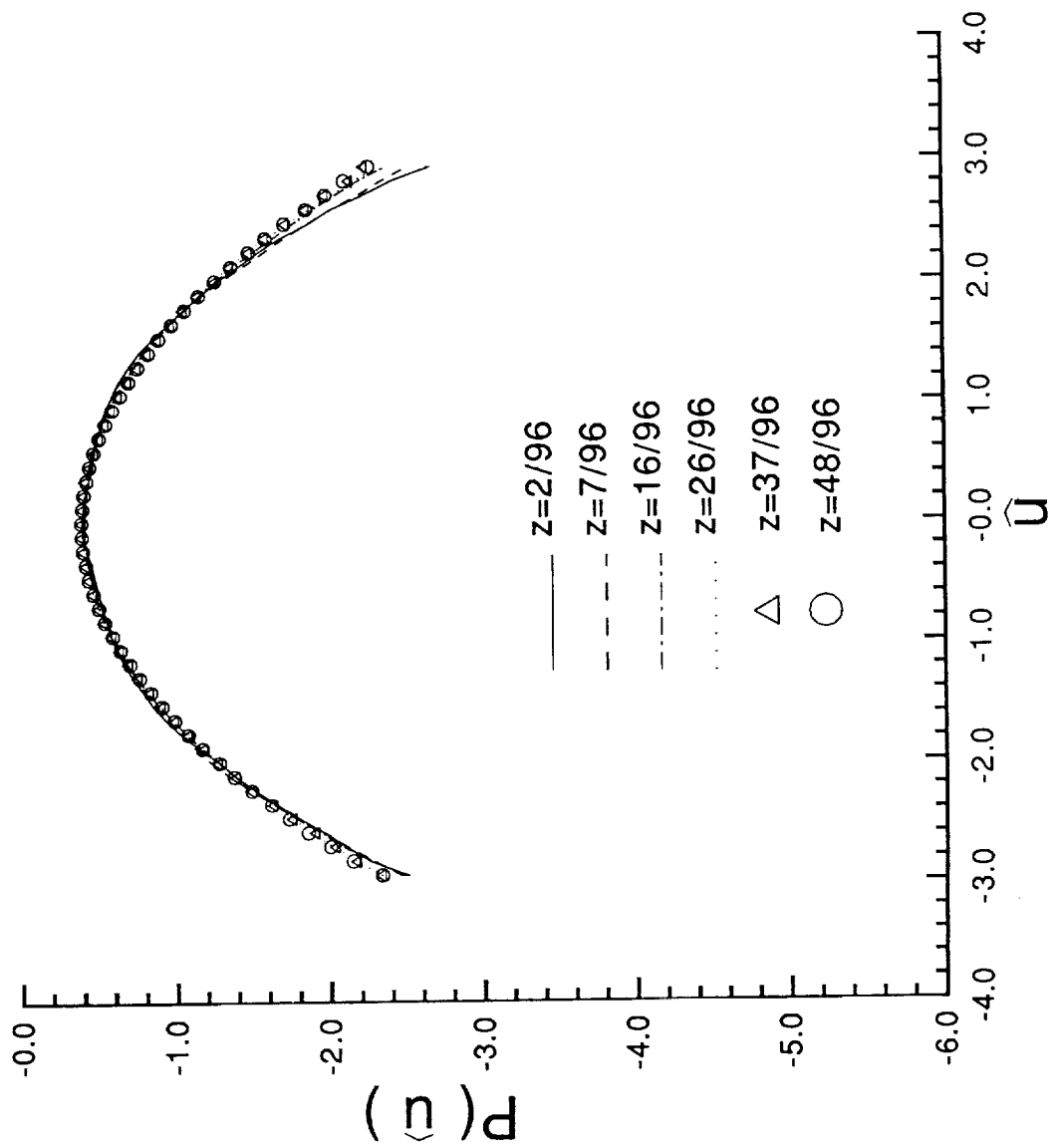


Figure 2a: Same as Fig. 1 but for  $\hat{u}$ .

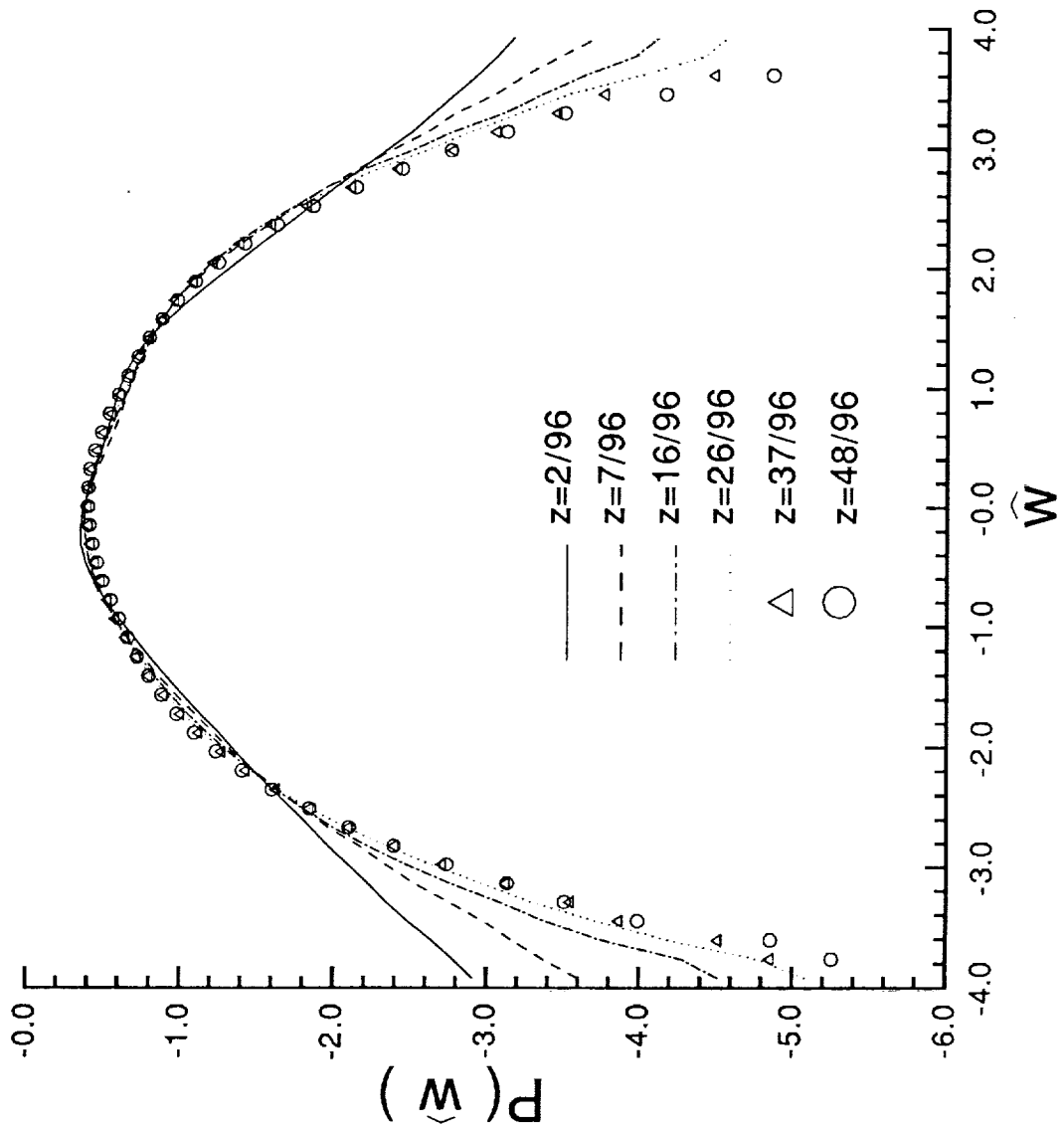


Figure 2b: Same as Fig. 1 but for  $\hat{w}$ .



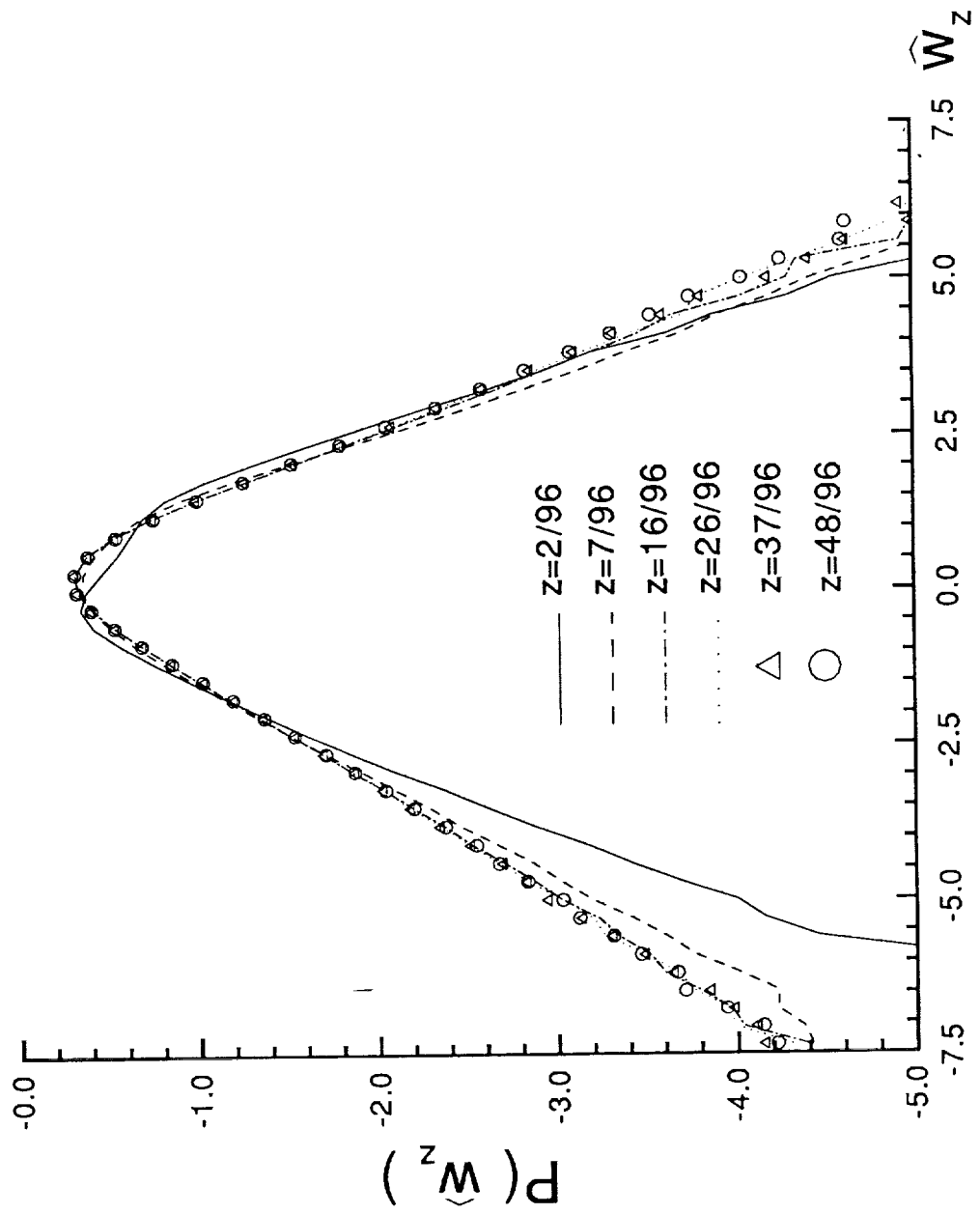


Figure 3a: Same as Fig. 1 but for  $\hat{w}_z$ .

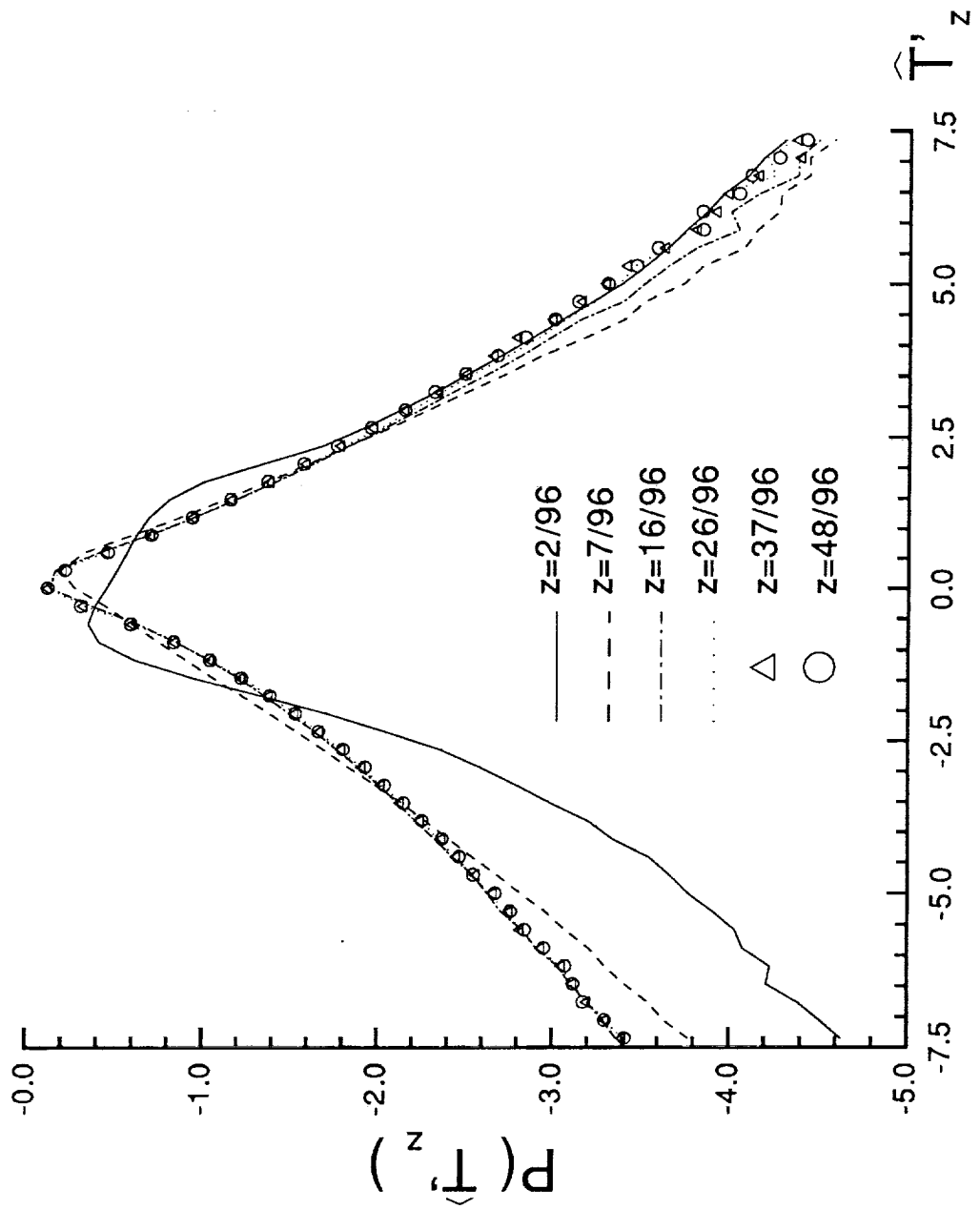


Figure 3b: Same as Fig. 1 but for  $\hat{T}_z$ .

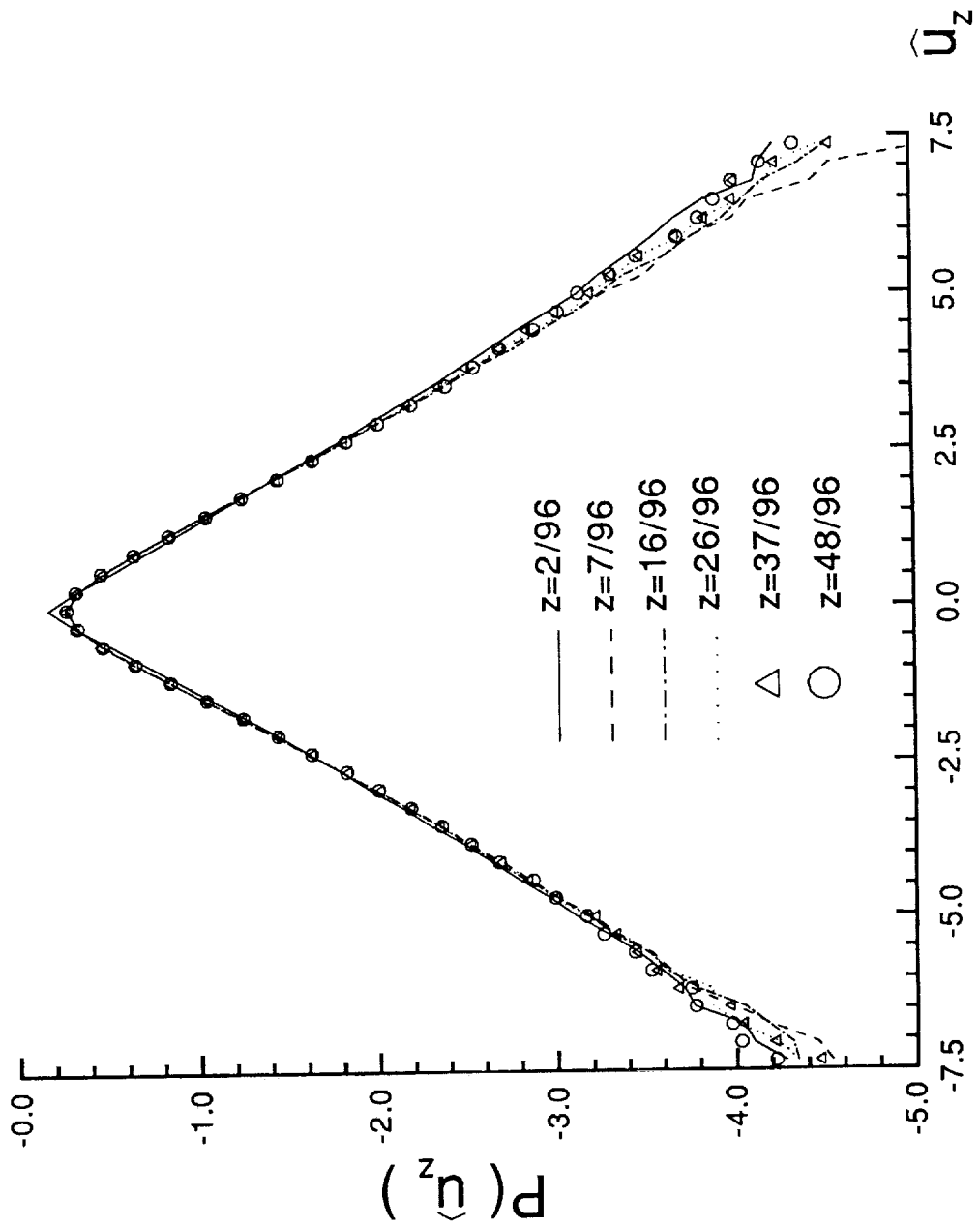


Figure 4: Same as Fig. 1 but for  $\hat{u}_z$ .

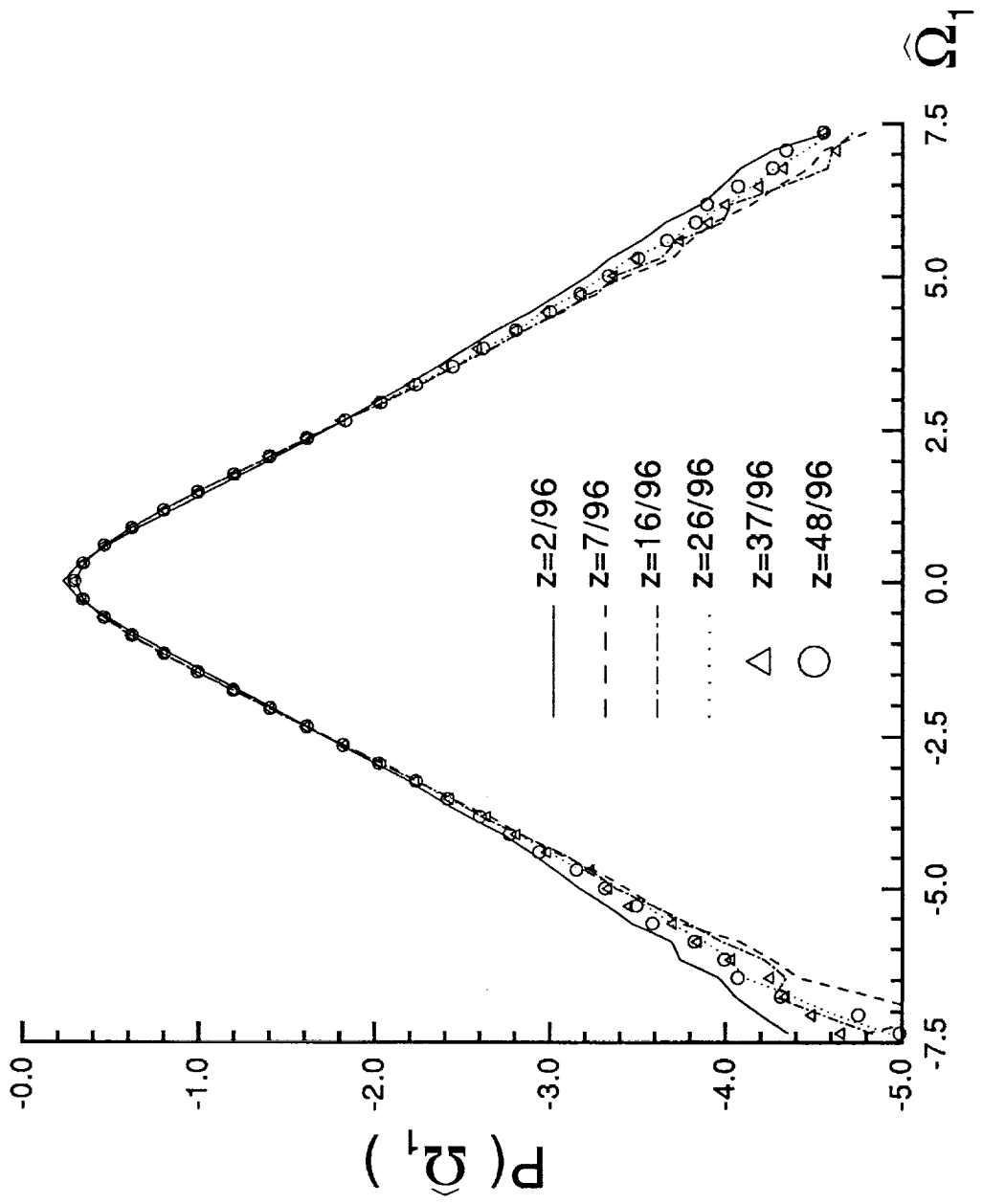


Figure 5a: Same as Fig. 1 but for  $\hat{\Omega}_1$ .

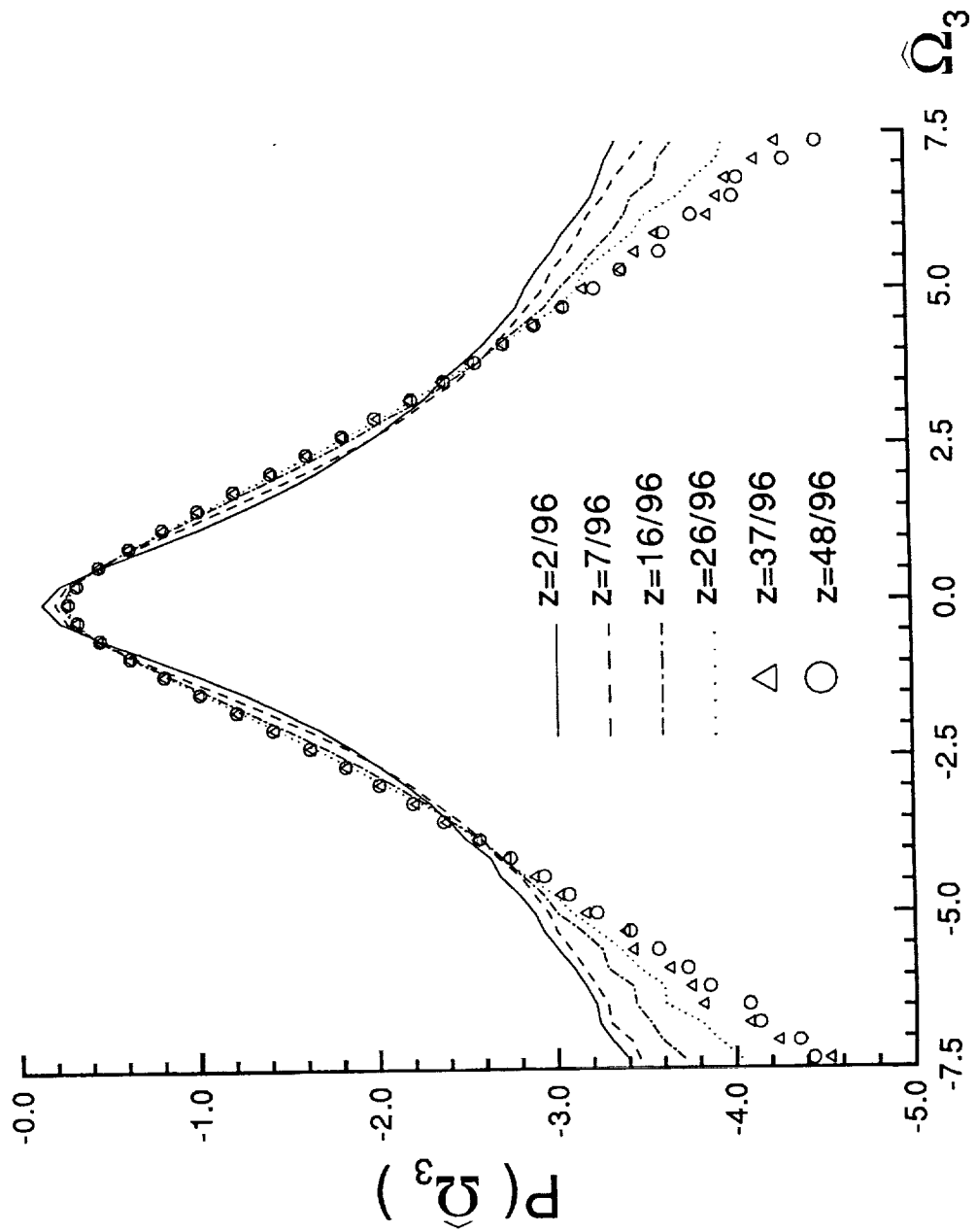


Figure 5b: Same as Fig. 1 but for  $\hat{\Omega}_3$ .

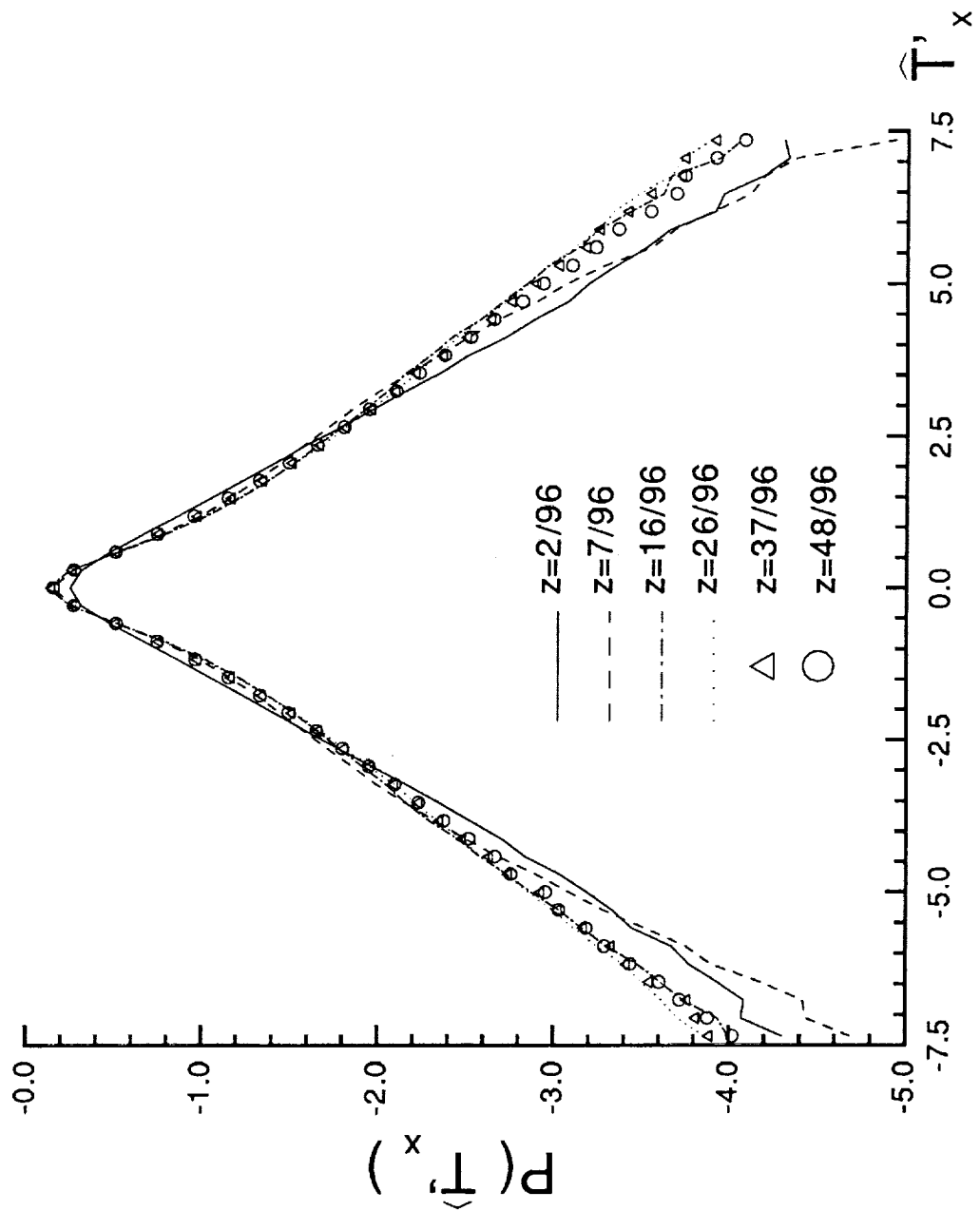


Figure 6: Same as Fig. 2 but for  $\hat{T}_x$ .

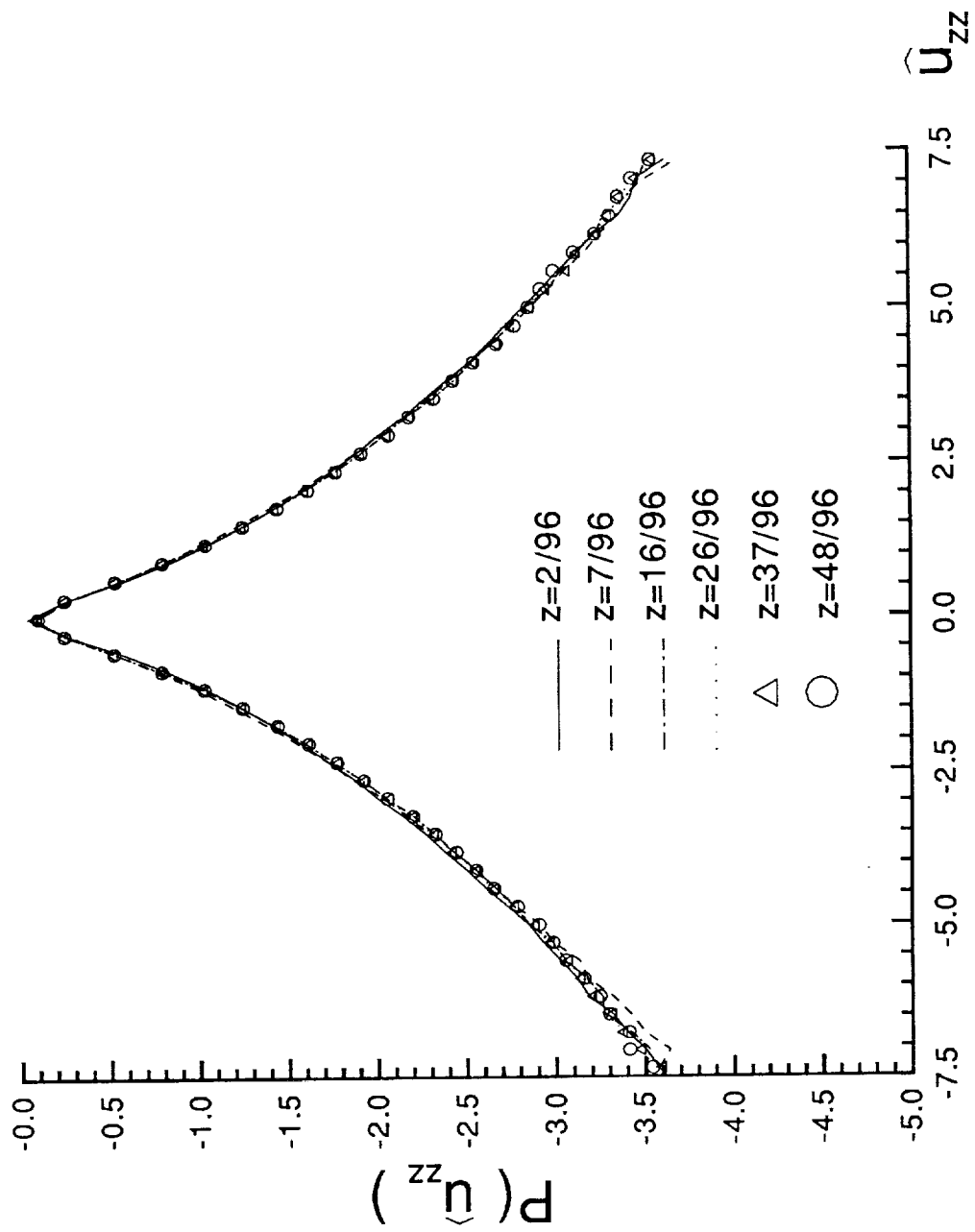


Figure 7a: Same as Fig. 1 but for  $\widehat{u}_{zz}$ .

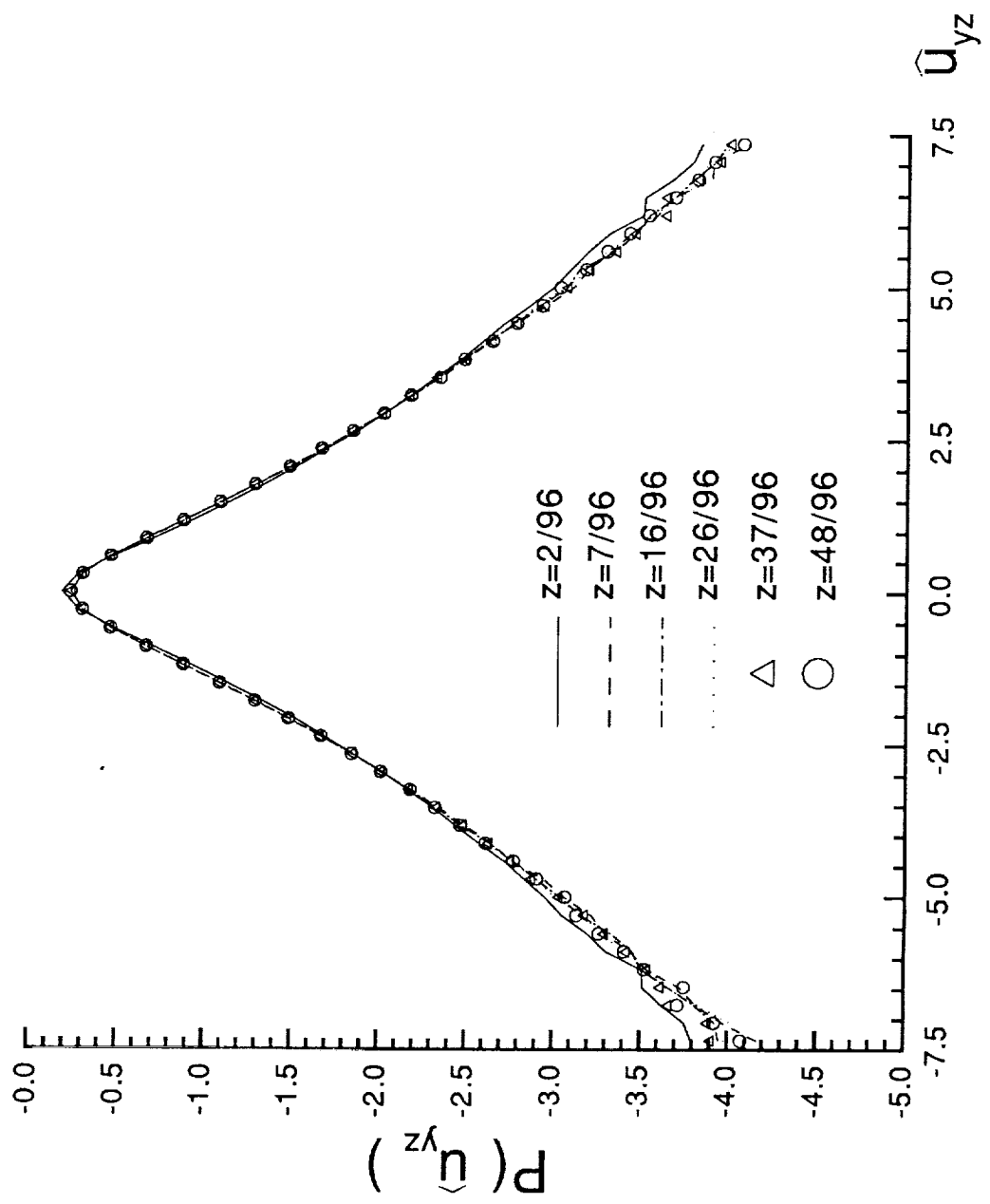


Figure 7b: Same as Fig. 1 but for  $\widehat{u}_{yz}$ .



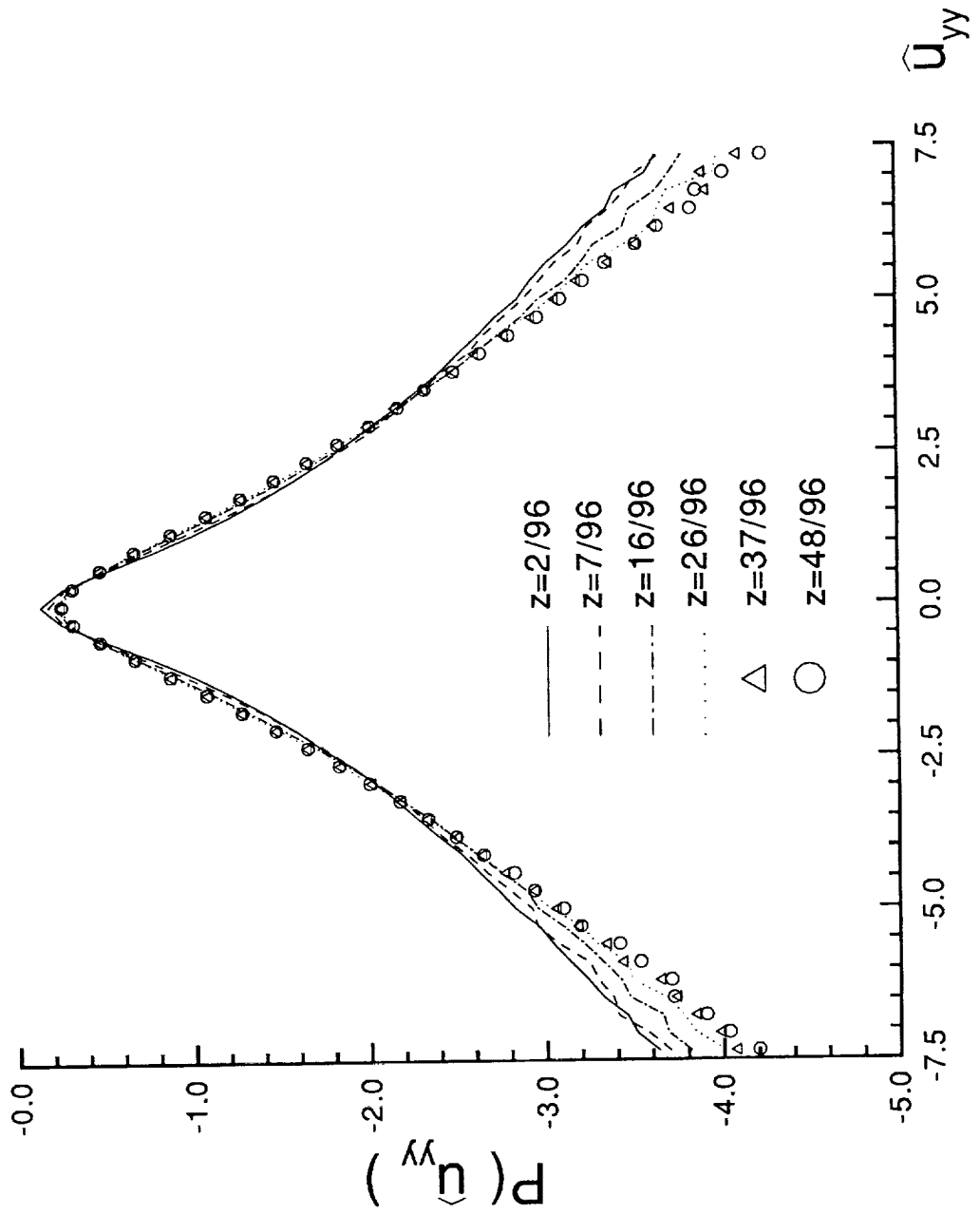


Figure 7c: Same as Fig. 1 but for  $\hat{u}_{yy}$ .

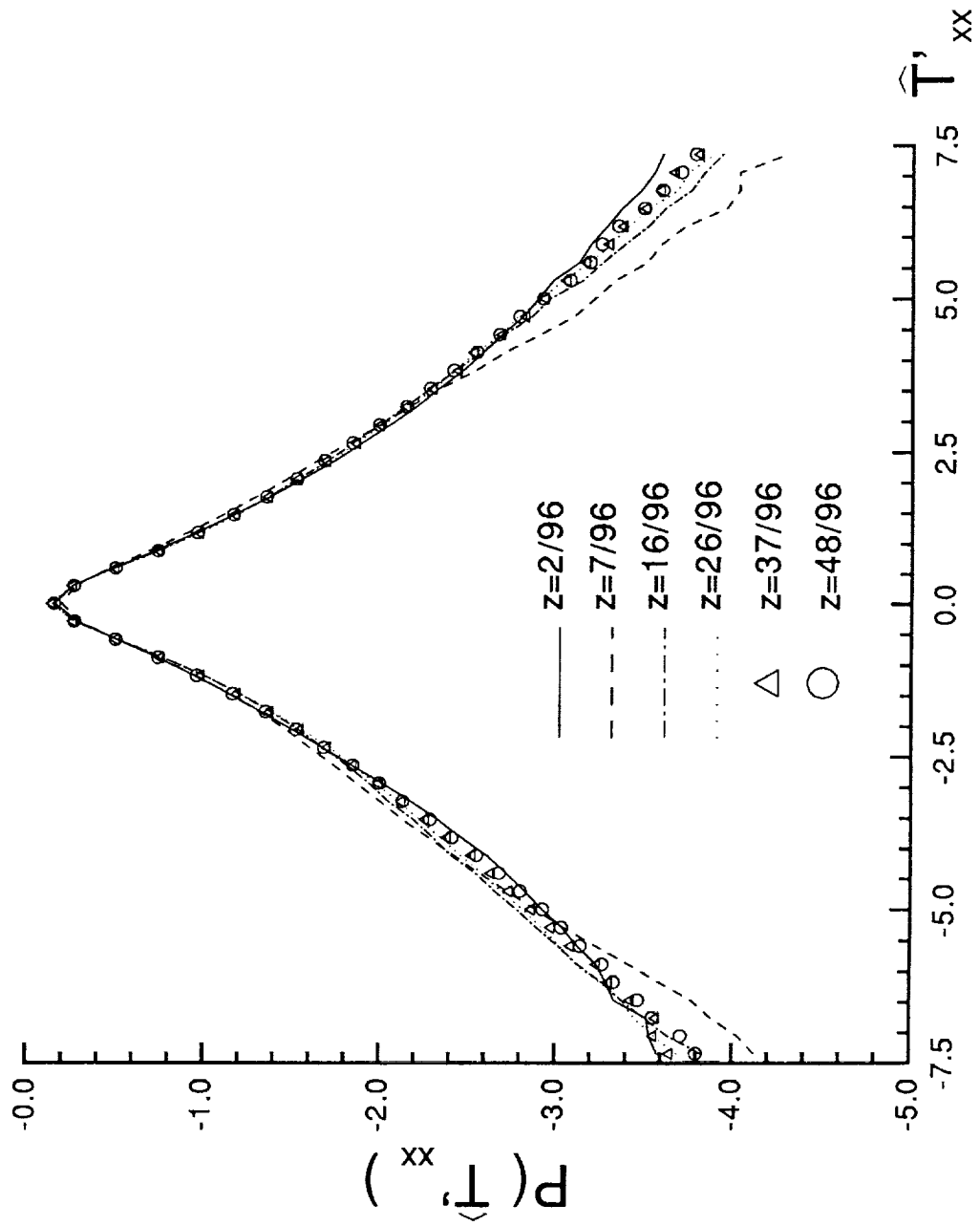


Figure 8a: Same as Fig. 1 but for  $\hat{T}'_{xx}$ .

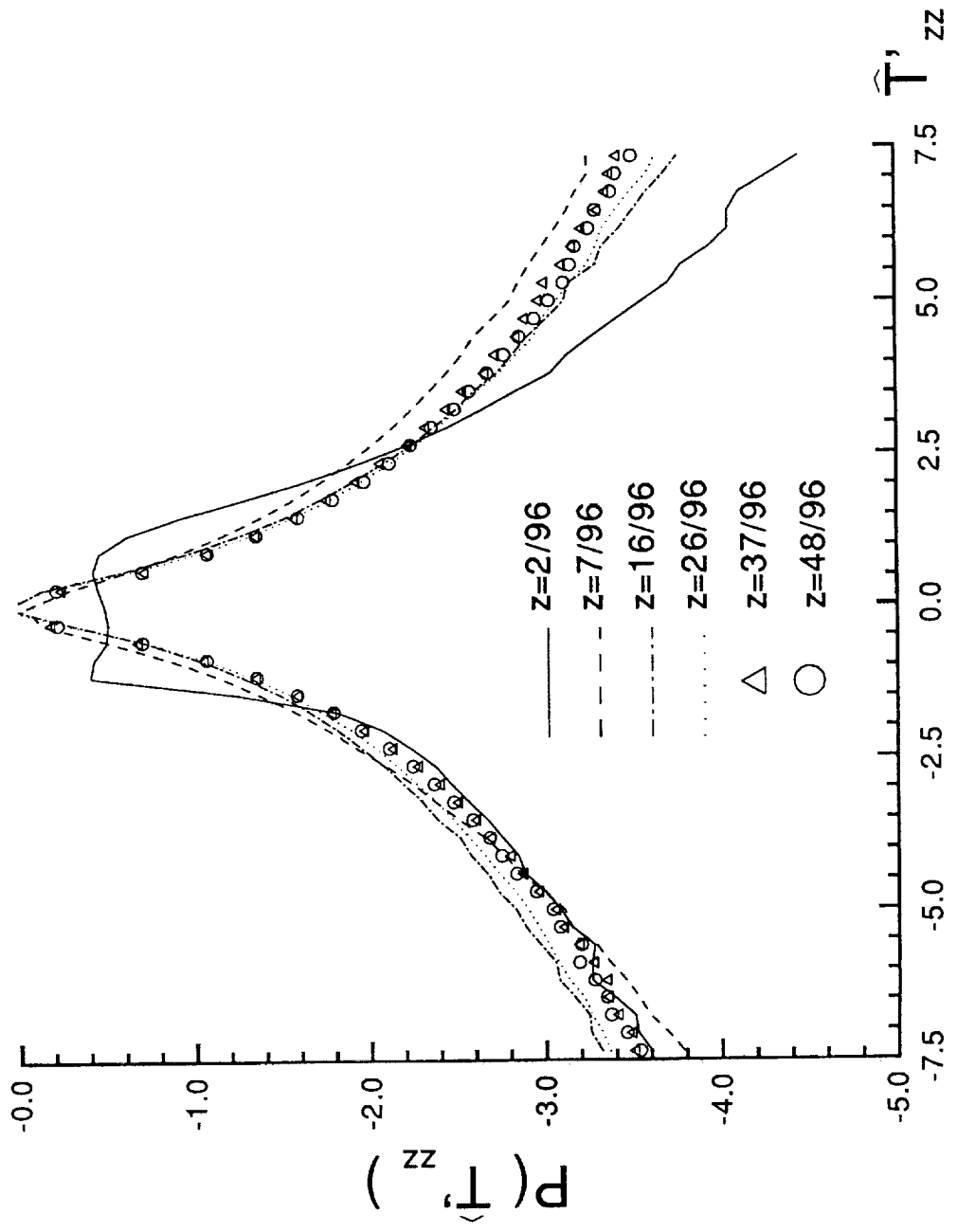


Figure 8b: Same as Fig. 1 but for  $\hat{T}_{zz}$ .

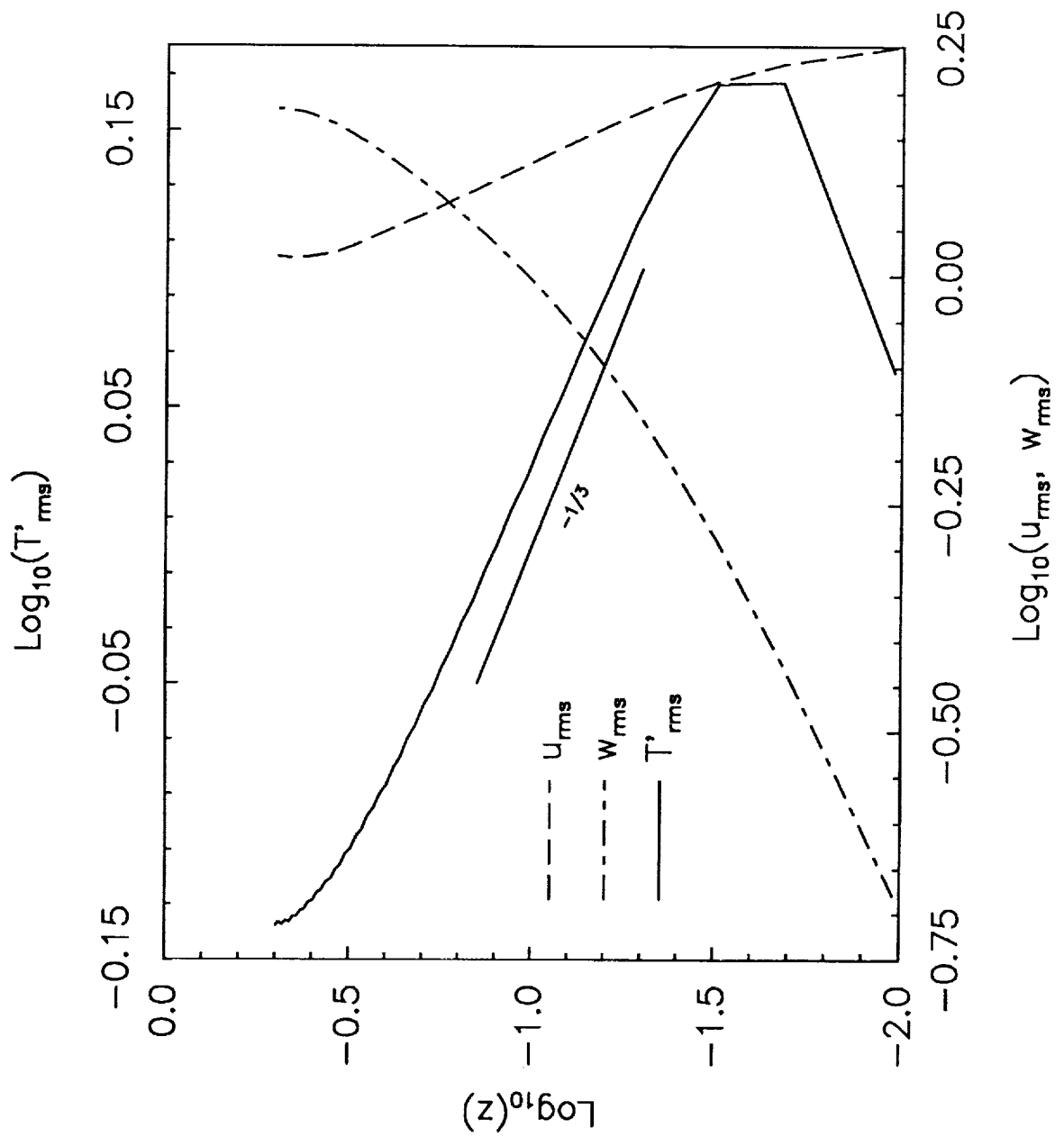


Figure 9a: A log-log plot of rms temperature, vertical velocity and horizontal velocity fluctuations against  $z$ . A straight line with  $-1/3$  slope is compared to  $T'_{rms}$ .

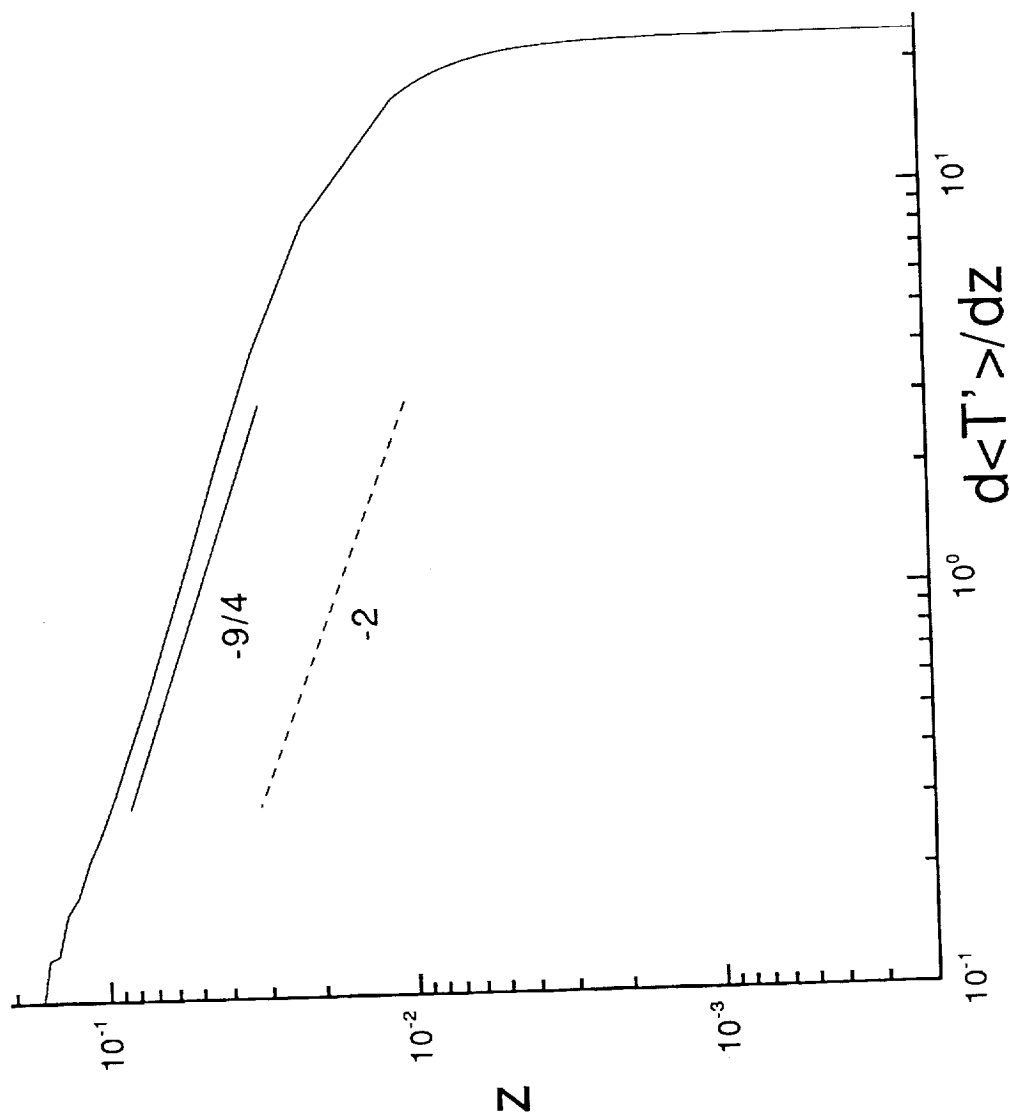


Figure 9b: A log-log plot of  $d \langle T' \rangle / dz$  against  $z$ . For comparison -2 and -9/4 slopes are also shown in this figure.

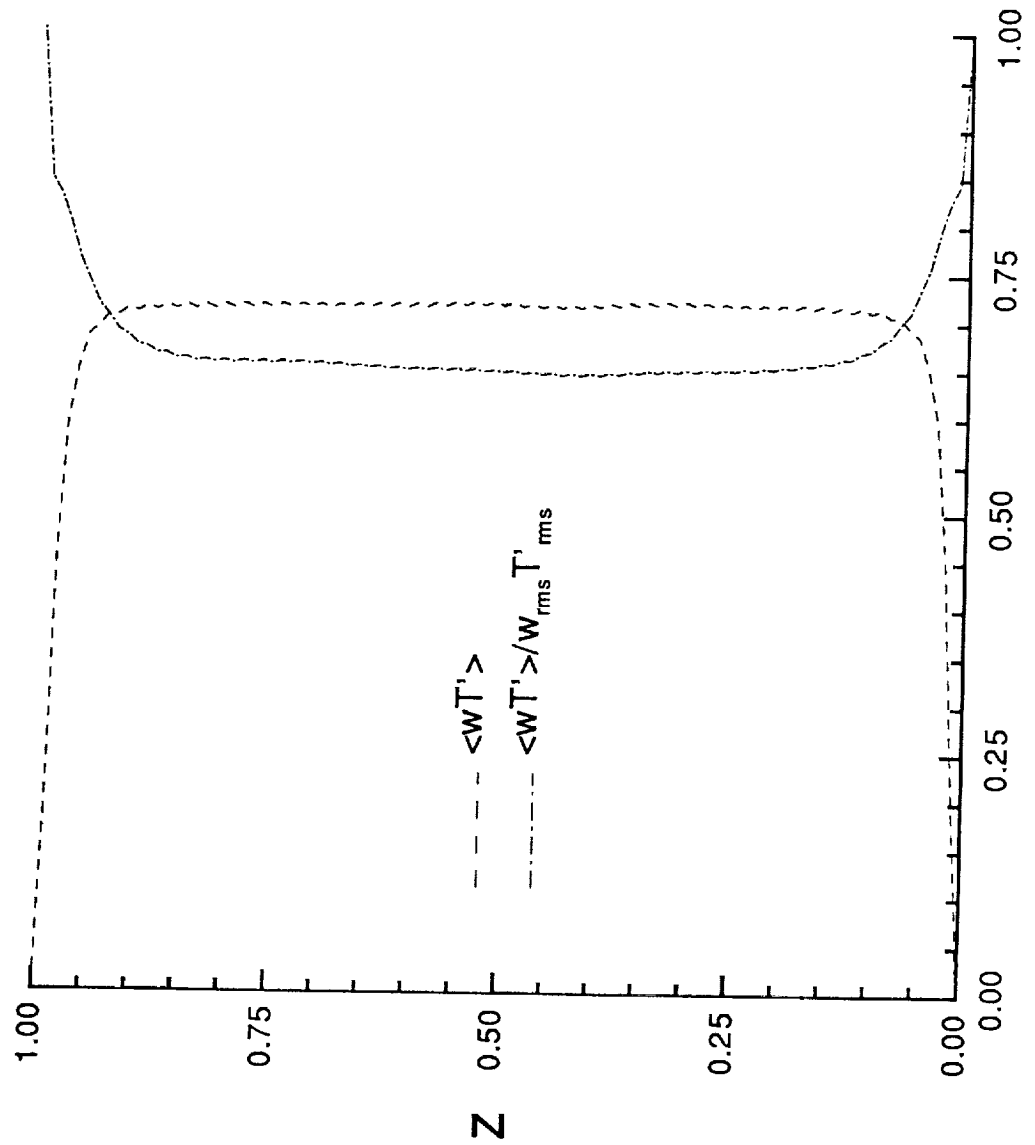


Figure 9c: Variation in  $wT'$  correlation and the covariance  $\langle wT' \rangle / w_{rms} T'_{rms}$  with respect to the vertical distance.

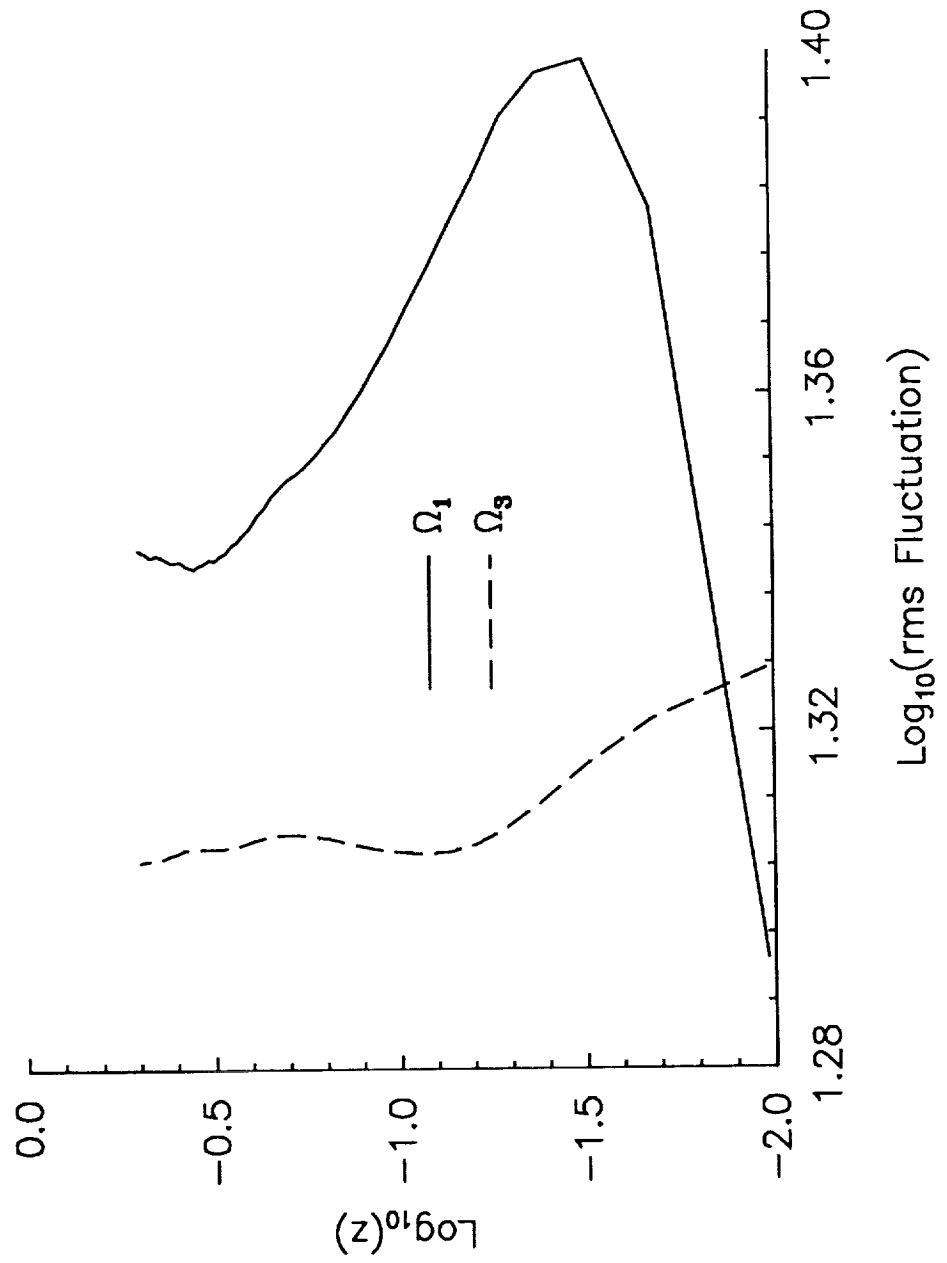


Figure 10: Log-log plot of rms fluctuation vorticity components  $\Omega_1$  and  $\Omega_3$ .

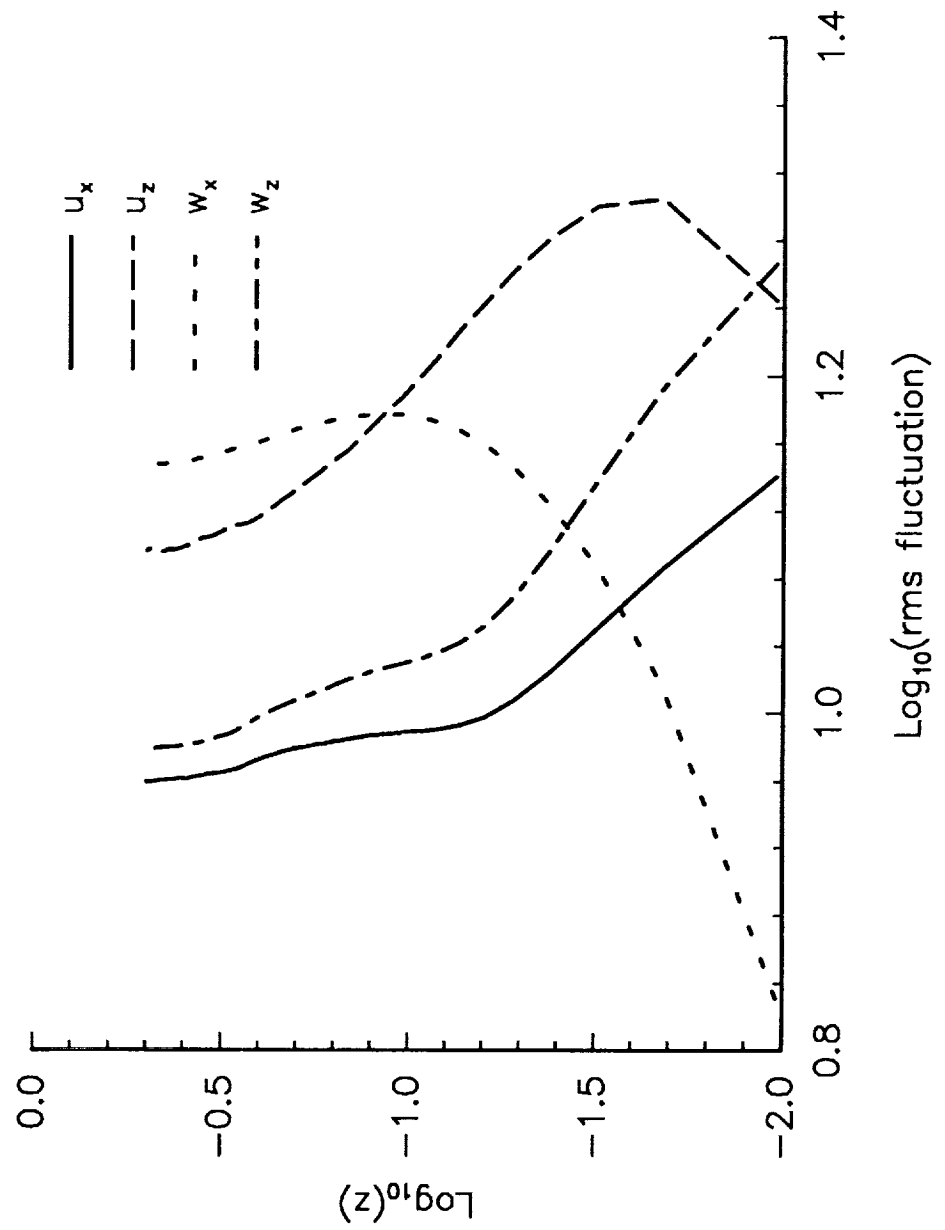


Figure 11: Rms fluctuation in  $u_x, u_z, w_x$  and  $w_z$  against vertical distance.



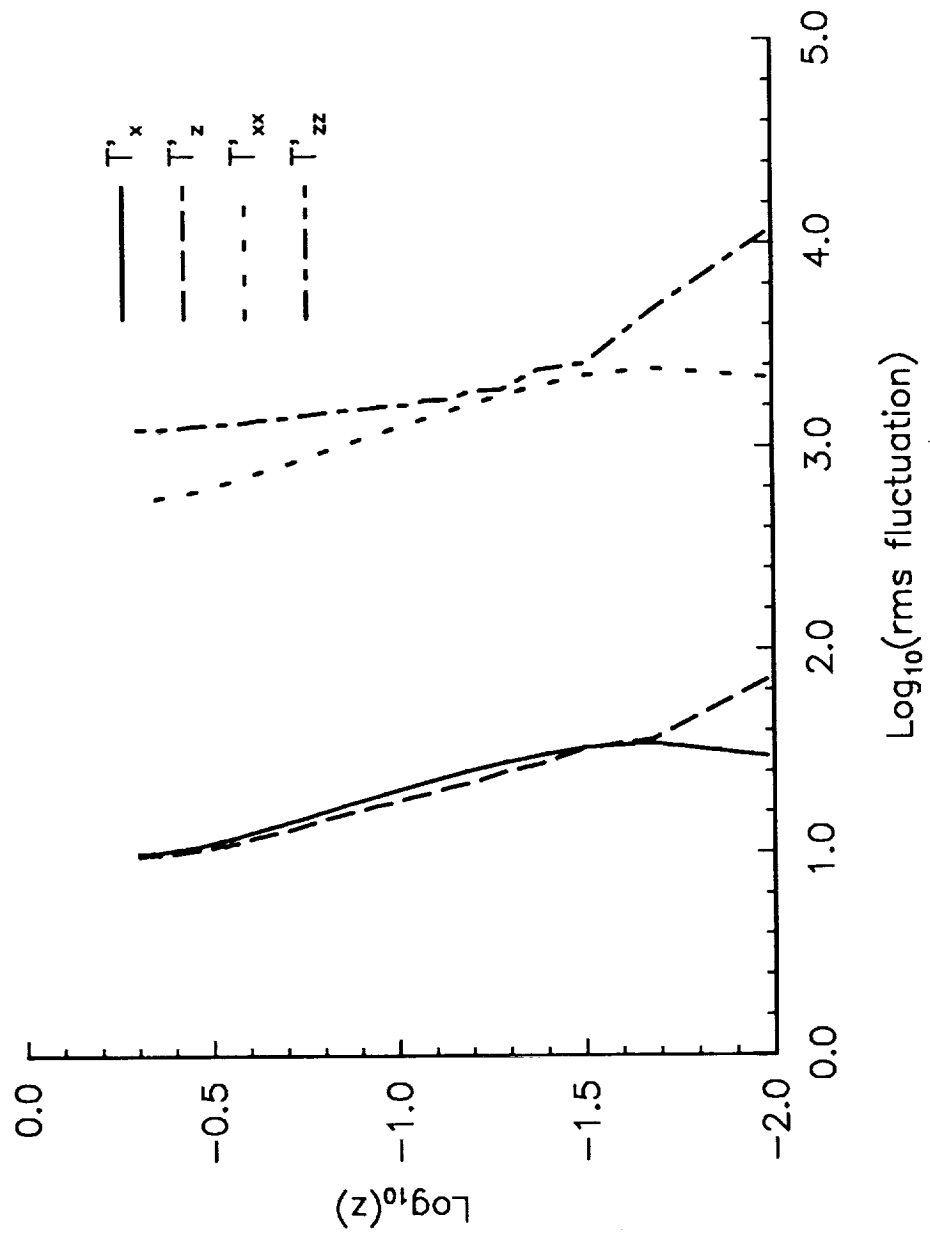


Figure 12: Rms fluctuation in  $T'_x, T'_z, T'_{xx}$  and  $T'_{zz}$  against vertical distance.

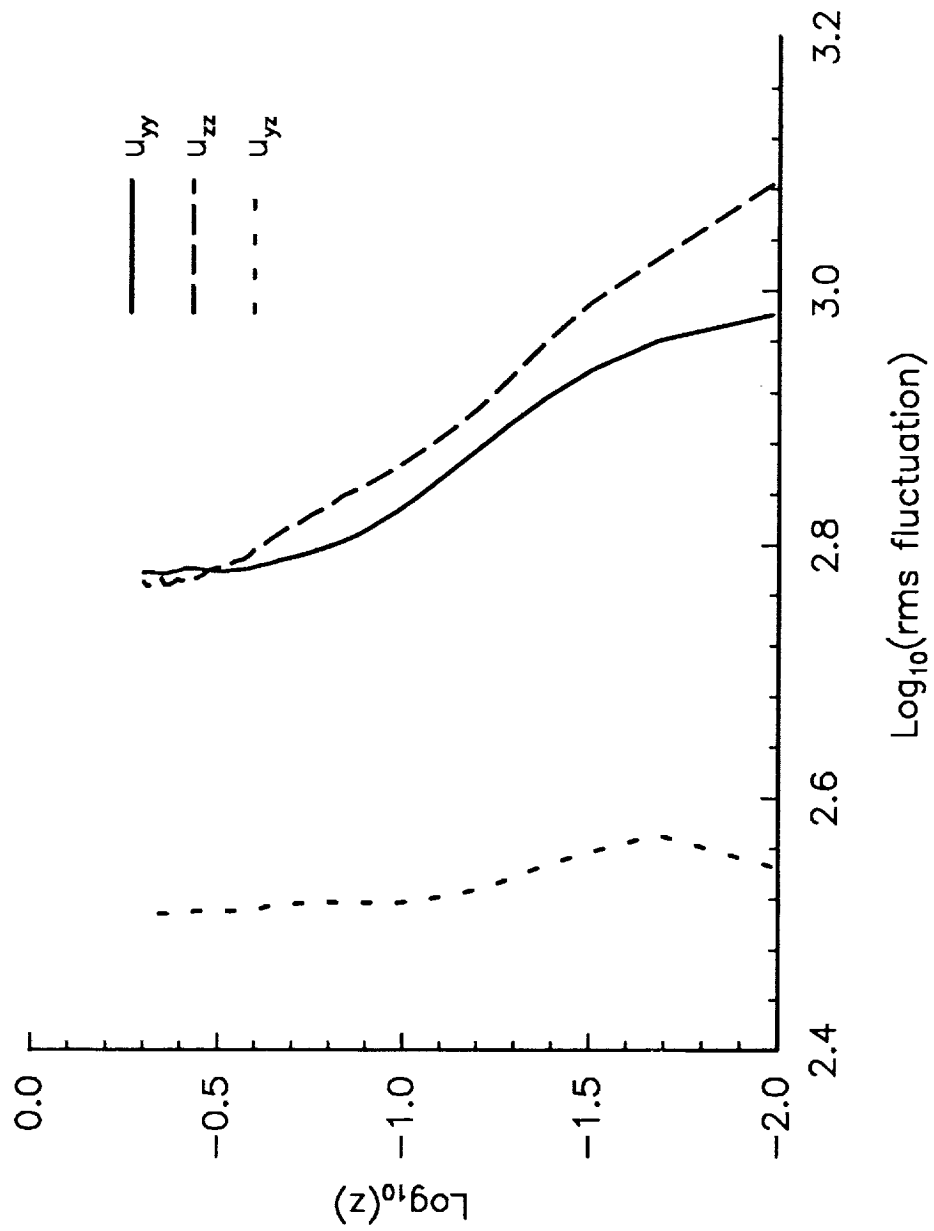


Figure 13: Rms fluctuation in  $u_{yy}$ ,  $u_{zz}$  and  $u_{yz}$  against vertical distance.







# Report Documentation Page

1. Report No. NASA CR-187519 ICASE Report No. 91-17		2. Government Accession No.		3. Recipient's Catalog No.	
4. Title and Subtitle  PROBABILITY DISTRIBUTION FUNCTIONS IN TURBULENT CONVECTION				5. Report Date February 1991	
				6. Performing Organization Code	
7. Author(s)  S. Balachandar L. Sirovich				8. Performing Organization Report No. 91-17	
				10. Work Unit No. 505-90-52-01	
9. Performing Organization Name and Address Institute for Computer Applications in Science and Engineering Mail Stop 132C, NASA Langley Research Center Hampton, VA 23665-5225				11. Contract or Grant No. NAS1-18605	
				13. Type of Report and Period Covered Contractor Report	
12. Sponsoring Agency Name and Address National Aeronautics and Space Administration Langley Research Center Hampton, VA 23665-5225				14. Sponsoring Agency Code	
15. Supplementary Notes Langley Technical Monitor: Michael F. Card Submitted to Physics of Fluids  Final Report					
16. Abstract  Results of an extensive investigation of probability distribution functions (pdfs) for Rayleigh-Bénard convection, in the hard turbulence regime, is presented. It is seen that the pdfs exhibit a high degree of internal universality. In certain cases this universality is established within two Kolmogorov scales of a boundary. A discussion of the factors leading to universality is presented.					
17. Key Words (Suggested by Author(s)) probability distributions, turbulent heat convection			18. Distribution Statement 34 - Fluid Mechanics and Heat Transfer 64 - Numerical Analysis  Unclassified - Unlimited		
19. Security Classif. (of this report) Unclassified		20. Security Classif. (of this page) Unclassified		21. No. of pages 40	22. Price A03

